Chap 9 Currents with Friction; Wind-driven Circulation

Wind is a major force driving oceanic currents. This has been well known for centuries.

9.1 Wind-driven circulation — introduction

The development of the theory of the wind-driven circulation

1. about 1898 Nansen explained qualitatively why wind-driven currents flow not in the direction of the wind but at 20^o to 40^o to the right of it (in the northern hemisphere);
2. in 1902 Ekman explained quantitatively for an idealized ocean how the rotation of the earth was responsible for the deflection of the current which Nansen had observed;
3. in 1947 Sverdrup showed how the main features of the equatorial surface currents could be attributed to the wind as a driving agent;
4. in 1948 Stommel explained the western intensification of the wind-driven circulation;
5. in 1950 Munk combined most of the above to obtain analytic expressions which described quantitatively the main features of the wind-driven circulation in terms of the real wind field;
6. in recent years, numerous numerical models have been developed for the circulation of individual ocean areas and for the world ocean.

Note: The theories described only the permanent (time-averaged) features of the flow. The variable part of the flow may have ten times the kinetic energy of the mean flow.

9.2 Nansen's qualitative argument

Nansen explained why icebergs in the Arctic drifted in a direction to the right of the direction of the wind at the sea surface, not in the direction of the wind itself (Fig. 9.1).

A steady state is reached in which $\vec{F}_t$ (wind friction), $\vec{F}_c$ (Coriolis force) and $\vec{F}_b$ (fluid friction) are in balance and the cube continues to move at a steady speed V_o in some direction between $\vec{F}_t$ and $\vec{F}_c$, i.e. to the right of the wind

direction (northern hemisphere).

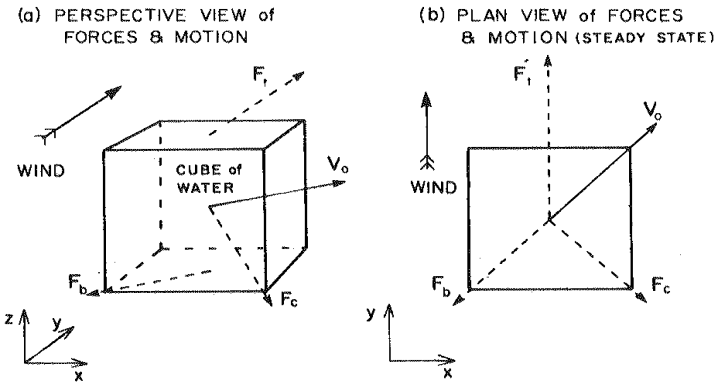

Fig. 9.1 Forces on a cube of water in the surface layer.

9.3 The equation of motion with friction included

$$\frac{du}{dt} = f\,v - \alpha\frac{\partial p}{\partial x} + F_x$$
$$\frac{dv}{dt} = -f\,u - \alpha\frac{\partial p}{\partial y} + F_y \qquad (9.1)$$

where F_x and F_y stand for the components of friction per unit mass.
If there are no accelerations (i.e. a steady state and zero advective accelerations), then $du/dt = dv/dt = 0$ and (9.1) becomes

$$f\,v + F_x - \alpha\frac{\partial p}{\partial x} = 0$$
$$-f\,u + F_y - \alpha\frac{\partial p}{\partial y} = 0 \qquad (9.2)$$

i.e. Coriolis + Friction + Pressure = 0 as shown schematically in Fig. 9.2.

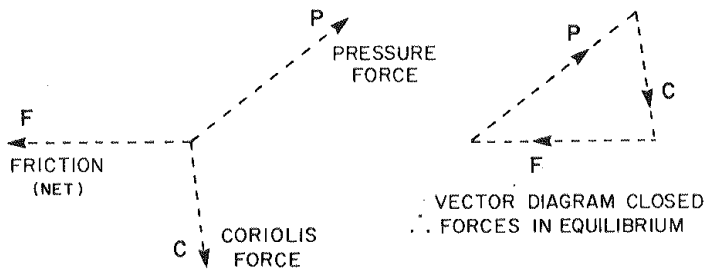

Fig. 9.2 Three forces in equilibrium on a water parcel.

Note: It differs from the geostrophic relationship in that the pressure and the Coriolis forces are no longer directly opposed.

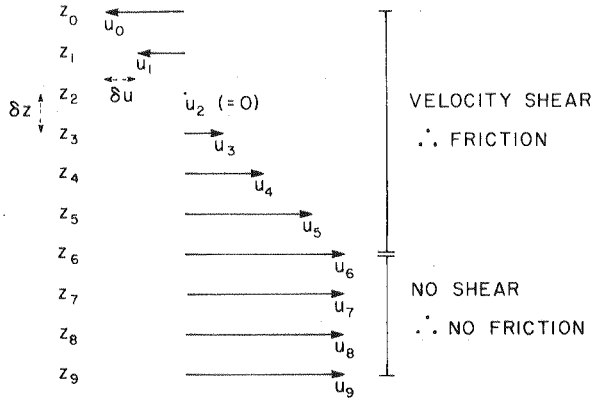

Fig. 9.3 Illustrating velocity shear and absence of shear.

Friction

In a fluid if two parts are in relative motion, friction will also occur. The two parts may be moving in opposite directions, or may be moving in the same direction with one going faster than the other (Fig. 9.3). In either case, there is said to be "velocity shear" ($\delta u/\delta z$) in the fluid and the value of the friction is related to this.

Newton's law of Friction states that

$$\tau = \mu \frac{\partial u}{\partial z} = \rho \upsilon \frac{\partial u}{\partial z} \tag{9.3}$$

The stress τ acts on the surface between the two layers which are moving at different speeds, tending to slow down the faster and to speed up the slower. Where μ is the coefficient of (molecular) ***dynamic*** viscosity ($\mu \sim 10^{-3}$ kg m^{-1}s^{-1}), and $\nu=\mu/\rho$ is the coefficient of (molecular) ***kinematic*** viscosity ($\nu \sim 10^{-6}$ m^{2}s^{-1}). In the ocean, the motion is generally turbulent. Thus, we use the eddy viscosity, which A_x, A_y of up to 10^5 m^{2}s^{-1} for horizontal shear (e.g. $\partial u/\partial y$, $\partial v/\partial x$) or of A_z of up to 10^{-1} m^{2}s^{-1} for the vertical shear (e.g. $\partial u/\partial z$).

So, the eddy friction stress $\tau=\rho A_z(\partial u/\partial z)$ expresses the force of one layer of fluid on an area of its neighbor above or below. In Fig. 9.4 a small cube of fluid is shown with shear in the *z*-direction and the required force would be $F=(\tau_2-\tau_1)\delta s$ in the *x*-direction.

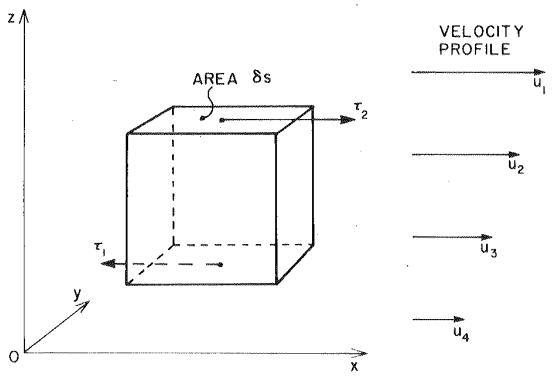

Fig. 9.4 For derivation of the friction term in the equation of motion.

$$\tau_2 = \tau_1 + \frac{\partial \tau}{\partial z}\delta z$$

$$\therefore (\tau_2 - \tau_1)\delta s = \frac{\partial \tau}{\partial z}(\delta s \delta z) = \frac{\partial \tau}{\partial z}(\delta V) \text{ where } \delta V\text{=volume of cube}$$

The force per unit volume = $\partial\tau/\partial z$

The force per unit mass = $\frac{1}{\rho}\frac{\partial \tau}{\partial z} = \alpha \frac{\partial \tau}{\partial z} = \alpha \frac{\partial}{\partial z}\left(\rho A_z \frac{\partial u}{\partial z}\right)$ (9.4)

Assume that A_z is constant, thus

$$\text{Friction force per unit mass} = A_z \frac{\partial^2 u}{\partial z^2} \quad (9.5)$$

Ekman's theory becomes

$$\begin{aligned} f v + A_z \frac{\partial^2 u}{\partial z^2} &= \alpha \frac{\partial p}{\partial x} \\ -f u + A_z \frac{\partial^2 v}{\partial z^2} &= \alpha \frac{\partial p}{\partial y} \end{aligned} \quad (9.6)$$

Scaling arguments:

Assume $A_z \sim 10^{-1}$ m^{2}s^{-1} $f = 10^{-4}$ s^{-1}

Compare friction with Coriolis forces

$$f u = A_z \frac{\partial^2 v}{\partial z^2}$$

$$f \mathrm{U} = A_z \frac{\mathrm{U}}{\mathrm{H}^2}$$

$$\mathrm{H} \approx 30 \text{ m}$$

i.e. Friction probably balances Coriolis force in the upper 30 m of the ocean.

9.4 Ekman's solution to the equation of motion with friction present

We can think of the velocity as having two parts (1) one associated with the horizontal pressure gradient and (2) one with vertical friction, i.e.

$$f v = f(v_g + v_E) = \alpha \frac{\partial p}{\partial x} - A_z \frac{\partial^2}{\partial z^2}(u_g + u_E) \quad (9.7)$$

where u_g, v_g are the geostrophic velocity components, $f v_g = \alpha \frac{\partial p}{\partial x}$ and

$f\,v_E = -A_z \dfrac{\partial^2 u_E}{\partial z^2}$, u_E, v_E are the Ekman velocity components associated with vertical shear friction (non-geostrophic).

The term $-A_z(\partial^2 u_g/\partial z^2)$ is neglected because it is $\leq 10^{-3}\alpha(\partial p/\partial x)$.

Ekman (1905) assumed that

(1) no boundaries

(2) infinitely deep water (to avoid the bottom friction term)

(3) A_z constant

(4) A steady wind blowing for a long time

(5) homogeneous water and the sea surface level so that $\partial p/\partial x = \partial p/\partial y = 0$ since density depends only on pressure, i.e. a barotropic condition and therefore there is no geostrophic flow

(6) f to be constant, i.e. the f-plane approximation

$$\left.\begin{aligned} f\,v_E + A_z \frac{\partial^2 u_E}{\partial z^2} &= 0 \\ -f\,u_E + A_z \frac{\partial^2 v_E}{\partial z^2} &= 0 \end{aligned}\right\} \quad \text{the Ekman equations} \qquad (9.8)$$

i.e. Coriolis + Friction = 0, as in Fig. 9.5(a).

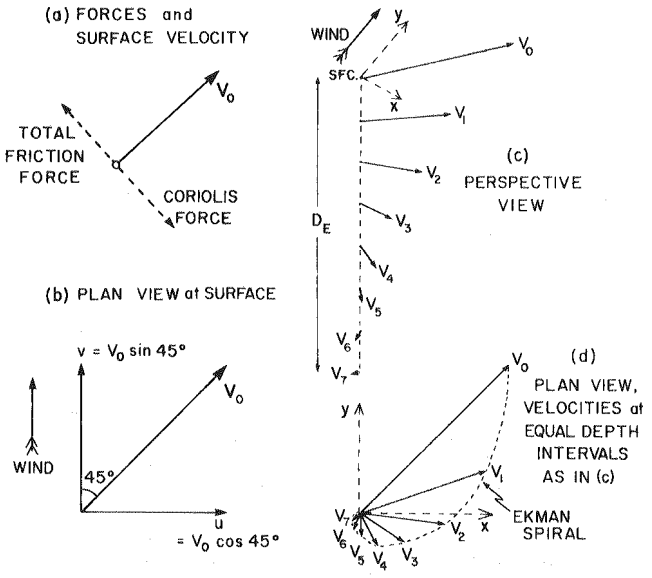

Fig. 9.5 Wind-driven currents from Ekman analysis: (a) net frictional stress balances Coriolis force with surface current $\vec{V}_0$ perpendicular to both; (b) wind in y–direction, surface velocity $\vec{V}_0$ and components; (c) perspective view showing velocity decreasing and rotating clockwise with increase in depth; (d) plan view of velocities at equal depth intervals, and the "Ekman spiral" (all for northern hemisphere).

If, for simplicity, we assume the wind to be blowing in the *y*-direction, the solutions to Ekman's equations are

$$u_E = \pm V_o \cos\left(\frac{\pi}{4} + \frac{\pi}{D_E} z\right) \exp\left(\frac{\pi}{D_E} z\right) \quad \text{(+ for northern hemisphere)}$$

$$v_E = V_o \sin\left(\frac{\pi}{4} + \frac{\pi}{D_E} z\right) \exp\left(\frac{\pi}{D_E} z\right)$$

where $V_o = \left(\sqrt{2}\pi\tau_{y\eta}\right) / \left(D_E \rho |f|\right)$ is the total Ekman surface current (9.10)

$\tau_{y\eta}$ = magnitude of the wind stress on the sea surface (approximately proportional to the wind speed squared and acting in the direction of the wind).

$|f|$ = the magnitude of *f*.

$D_E = \pi(2A_z/|f|)^{1/2}$ is the ***Ekman depth*** or ***depth of friction influence***.

Note: The following is the derivative of the Ekman solution.

From (9.8), we assume that $w = u + i\,v$. So

$$\frac{\partial^2 w}{\partial z^2} = \frac{\partial^2 u}{\partial z^2} + i\frac{\partial^2 v}{\partial z^2} = -\frac{f\,v}{A_z} + i\frac{f\,u}{A_z} = \frac{i\,f}{A_z}(u + i\,v) = \frac{i\,f}{A_z} w$$

We can obtain

$$w = A_1\, e^{(i\,f/A_z)^{1/2} z} + A_2\, e^{-(i\,f/A_z)^{1/2} z}$$

Boundary conditions:

(1) $z \to -\infty$, $u = v = 0$

(2) $\tau = \rho A_z \frac{\partial w}{\partial z} = \rho A_z \left(\frac{\partial u}{\partial z} + i\frac{\partial v}{\partial z}\right) = \tau_x + i\,\tau_y$, at z = 0, $\tau = i\ \tau_y$

(a) For $z \to -\infty$, $w = u + i\,v \Rightarrow A_2 = 0$ and $w = A_1\, e^{(i\,f/A_z)^{1/2} z}$

(b) For $z = 0$, $A_z \rho \frac{\partial w}{\partial z} = A_z \rho A_1 \left(\frac{if}{A_z}\right)^{1/2} e^{(if/A_z)^{1/2} z} = \tau = \tau_x + i\,\tau_y$

$$\rho A_z A_1 \sqrt{\frac{if}{A_z}} = i\,\tau_y \qquad \Rightarrow \qquad A_1 = \frac{i\,\tau_y}{\rho A_z (if/A_z)^{1/2}} = \frac{\tau_y \sqrt{i}}{\rho \sqrt{A_z f}}$$

$$\text{Note}: \quad i = \cos(\frac{\pi}{2} + 2k\pi) + i\sin(\frac{\pi}{2} + 2k\pi)$$
$$i^{1/2} = \cos(\frac{\pi}{4} + k\pi) + i\sin(\frac{\pi}{4} + k\pi)$$
$$e^{i\theta} = \cos\theta + i\sin\theta$$

$$w = \frac{\tau_y\sqrt{i}}{\rho\sqrt{A_z f}} e^{\sqrt{\frac{f}{A_z}}\left(\frac{1}{\sqrt{2}}+\frac{i}{\sqrt{2}}\right)z} \qquad \left(\text{Let } \sqrt{\frac{f}{2A_z}} = \frac{\pi}{D_E} \quad \Rightarrow \quad D_E = \pi\sqrt{\frac{2A_z}{f}}\right)$$

$$w = \frac{\tau_y\sqrt{i}}{\rho\sqrt{A_z f}} e^{\frac{\pi}{D_E}(1+i)z} = \frac{\pi\sqrt{2}\tau_y\sqrt{i}}{\rho\pi\sqrt{2A_z/f}\,f} e^{\frac{\pi}{D_E}(1+i)z} = \frac{\sqrt{2}\pi\tau_y}{\rho D_E f}\sqrt{i}\, e^{\frac{\pi}{D_E}(1+i)z}$$
$$= V_o e^{\frac{\pi}{4}i} e^{\frac{\pi}{D_E}z} e^{i\frac{\pi}{D_E}z} = V_o e^{\frac{\pi}{D_E}z} e^{(\frac{\pi}{4}+\frac{\pi z}{D_E})i}$$
$$= V_o e^{\frac{\pi}{D_E}z}\cos(\frac{\pi}{4} + \frac{\pi}{D_E}z) + iV_o e^{\frac{\pi}{D_E}z}\sin(\frac{\pi}{4} + \frac{\pi}{D_E}z)$$
$$= u + iv$$

Interpretation of these solutions:

(1) At the sea surface where $z = 0$, the solution become

$$u = \pm V_o\cos 45^o, \qquad v = V_o\sin 45^o$$

which means that the surface current flows at 45° to the right (left) of the wind direction in the northern (southern) hemisphere.

(2) Below the surface, where z is no longer zero, the total current speed = $V_o \exp(\pi z/D_E)$ becomes smaller as depth increase, i.e. as z becomes more negative, while the direction changes clockwise (anticlockwise) in the northern (southern) hemisphere.

(3) The direction of the flow becomes opposite to that at the surface at $z = -D_E$ where the speed has fallen to $\exp(-\pi)=0.04$ of that at the surface. The depth D_E is usually arbitrarily taken as the effective depth of the wind-driven current, the ***Ekman layer***. When viewed in plan, the tips of the current vector arrows form a decreasing spiral called the "Ekman current spiral" (Fig. 9.5(d)).

Note: The assumption is made in that the wind was blowing along the

y-direction to keep the solutions relatively simple as shown above. If the wind is blowing in some other direction the current pattern will be the same relative to the wind direction.

In order to obtain numerical relations between the surface current (V_o), the wind speed (W), and the depth (D_E), Ekman made 2 observations:

Obs 1: The wind stress magnitude $\tau_\eta = \rho_a C_D W^2$ where ρ_a = the density of air, the drag coefficient $C_D \cong 1.4 \times 10^{-3}$ (non-dimensional), and W is the wind speed in ms^{-1}. Then $\tau_\eta = 1.3$ kg m$^{-3} \times 1.4 \times 10^{-3} \times W^2 = 1.8 \times 10^{-3} W^2$ Pa.

$$V_o = \frac{\sqrt{2} \times \pi \times 1.8 \times 10^{-3} \times W^2}{D_E \times 1025 \,\text{kgm}^{-3} \times |f|} = 0.79 \times 10^{-5} \frac{W^2}{D_E |f|} \,\text{m s}^{-1} \qquad (9.11)$$

Obs 2: Field observations analyzed by Ekman indicate that the surface current and the wind speed are related as

$$\frac{V_o}{W} = \frac{0.0127}{(\sin|\phi|)^{1/2}} \quad \text{outside } \pm 10^o \text{ latitude from the equator.} \qquad (9.12)$$

Then, $$D_E = \frac{4.3W}{(\sin|\phi|)^{1/2}} \quad \text{meters (with } W \text{ in m s}^{-1}) \qquad (9.13)$$

If we know W at latitude ϕ we can calculate (1) V_o and D_E, then (2) from D_E we can estimate the eddy viscosity A_z.

Table 9.1 Some values for D_E and estimate A_z

Latitude	$\phi = 10^o$	45^o	80^o	
V_o/W	$= 0.030$	0.015	0.013	A_z
Wind speed (W)				(estimated)
10 m s^{-1}	D_E=100	50	45 m	0.0014 m^{2}s^{-1}
20	=200	100	90	0.055

9.41 Comments on the experimental observations used by *Ekman*

Note:

(1) Obs. 1 and 2 are reasonable but not exact. For instance, there is variability in the value of C_D, the present estimates suggesting values from 1.3 to 1.5 $\times$ $10^{-3} \pm 20\%$, for wind speeds up to about 15 m s^{-1}.

(2) The constant in Ekman's expression (9.12) for V_o/W probably overstates its accuracy because more extensive data yield values ranging from 2 to 5% in

mid-latitudes. In addition, time-dependent effects and the mixed-layer depth are probably important.

(3) Very often, D_E has been estimated from or compared with the depth of the upper mixed layer, although the assumption that this "mixed- layer depth" is identical with the Ekman depth is not correct very often. Because the mixed-layer depth depends on

   (a) the past history of the wind in the locality rather more than on the wind speed at the time of observation.

   (b) the stability of the underlying water and on the heat balance through the surface (which determines convective effects).

(4) The formation of the mixed layer is a complicated time-dependent process, which is still not fully understood.

(5) One would expect the Ekman depth to be rather less than the mixed-layer depth in most cases, because the latter may be much influenced by even short periods of strong winds. It follows that A_z , which is calculated from D_E are, in general, probably too large.

(6) The mean features of the current turning to the right and decreasing with depth are probably correct, but the details are not to be taken too seriously. Because there are very few measured current profiles which are adequate to test the theory. It is difficult to make accurate current measurements in the open, deep ocean the only region where the Ekman theory applies, and difficult to get sufficiently steady wind conditions.

(7) A version of the Ekman theory also applies to the velocity structure in the atmosphere above the earth's surface and there are some observations to show that the theory applies fairly well in this case. This layer is referred to as the ***planetary boundary*** or ***Ekman layer***, or sometimes as the ***region of frictional influence***.

9.42 Transport and upwelling — the effect of boundaries

The wind-driven Ekman current has its maximum speed at the surface and the speed decreases with depth increase. So, the net transport will be to the right of the wind direction in the northern hemisphere, in fact it will be shown to be at ***right angles*** to the wind direction.

Eqs. (9.6) in the absence of any pressure gradient can written as

$$\rho f v_E \, dz = -d\tau_x \qquad\qquad -\rho f u_E \, dz = -d\tau_y \tag{9.14}$$

(1) $\rho\, v_E\, dz$ is the mass flowing per second in the *y*-direction through a vertical area of depth *dz* and width 1 m in the *x*-direction.

(2) $\int_z^{\circ} \rho\, v_E\, dz$ will be the total mass flowing in the *y*-direction from the level *z* to the surface for this strip 1 m wide. $\int_z^{\circ} \rho\, u_E\, dz$ will be the total mass transport per unit width in the *x*-direction.

(3) If we choose $z = -2\, D_E$ where the speed will be $\exp(-2\pi) = 0.002$ of that at the surface, i.e. substantially zero.

$$\begin{aligned} f\, M_{yE} &= f \int_{-2D_E}^{\circ} \rho\, v_E\, dz = -\int_{-2D_E}^{\circ} d\tau_x = -(\tau_x)_{sfc} + (\tau_x)_{-2D_E} \\ f\, M_{xE} &= f \int_{-2D_E}^{\circ} \rho\, u_E\, dz = \int_{-2D_E}^{\circ} d\tau_y = (\tau_y)_{sfc} - (\tau_y)_{-2D_E} \end{aligned} \qquad (9.15)$$

$(\tau_x)_{-2D_E}$ and $(\tau_y)_{-2D_E}$ will be essentially zero because the velocity below the wind-driven layer is substantially zero and therefore there can be no shear and therefore no friction. So we have

$$f\, M_{xE} = \tau_{y\eta} \quad \text{and} \quad f\, M_{yE} = -\tau_{x\eta} \qquad (9.16A)$$

where the subscript η indicates surface values.

Alternative forms of (9.16A) are

$$f\, Q_{xE} = \alpha\, \tau_{y\eta} \quad \text{and} \quad f\, Q_{yE} = -\alpha\, \tau_{x\eta} \qquad (9.16B)$$

where $Q_y = \int_z^{\circ} v_E\, dz$ is the volume transport (per unit width).

In our example, where the wind is entirely in the *y*-direction, $\tau_{x\eta} = 0$ and therefore $M_{yE} = 0$, but $M_{xE} > 0$ because $\tau_{y\eta} > 0$, showing that the net transport is to the right of and at right angles to the wind direction.

Discussions:

(1) For Ekman's infinite ocean, there is inflow from the left of the wind direction to replace the flow away to the right.

(2) If the wind is blowing parallel to a coastline which is on the left of the wind, the wind causes the surface or Ekman layer to move to the right, i.e. away from the coast. So, water from ***below*** the surface comes up to replace it. This behavior is called ***upwelling*** and the region near the coast is one of the ***divergence***.

(3) This phenomenon occurs at times along many regions of the eastern sides of the oceans. In the northern hemisphere, the wind must blow along the coast in a southerly direction, which usually happens during the summer. In the southern hemisphere, the transport is to the left of the wind and so it must blow in a northerly direction for upwelling to occur.

(4) The upwelled water does not come from great depths. Studies of the properties of the upwelled water indicate that it comes from depths not greater than 200-300 m. When the upwelled water has high nutrient, plankton production may be promoted and the process is therefore important biologically.

(5) If the wind blows away from the equator along the eastern boundary of an ocean, then water will be forced toward the coast and the level will rise. This process may then give rise to a surface slope and a consequent ***geostrophic*** current.

(6) In upwelling region also, a surface slope is usually caused, in this case down toward coast. The induced geostrophic currents along the coast generally have considerably higher speed than the wind-induced (Ekman) onshore-offshore currents, making the latter difficult to measure. On the eastern side of an ocean, the downward slope toward the coast requires an equatorward flow at the surface if the pressure gradient is to be balanced, at least in the main, by the Coriolis force. We say "in the main" because near shore and/or in shallow water friction is likely to become important and the current may not be purely geostrophic.

(7) As the density of the water near the coast is higher than that offshore at the same level, ***baroclinic*** compensation will occur, i.e. the long- shore flow will decrease with depth. Sometimes "overcompensation" may occur and the offshore pressure gradient changes sign at depth, requiring a poleward undercurrent to provide a balancing (or partially balancing) Coriolis force.

9.43 Upwelling and downwelling away from boundaries

If the wind remains constant in direction but varies in speed across the direction of the wind, then the Ekman transport perpendicular to the wind will vary and the upper-layer waters will be forced toward or away from each other, i.e. convergences or divergences will develop. Continuity then requires that a convergence be accompanied by downward motion (downwelling) while a divergence will be accompanied by upward motion (upwelling).

For example, in the North Atlantic the general direction of the wind is to the east at higher latitudes ("westerlies" meaning the wind from west) and to the west at lower latitudes ("easterlies"). Fig. 9.6(a) shows the mean winds in simplified form.

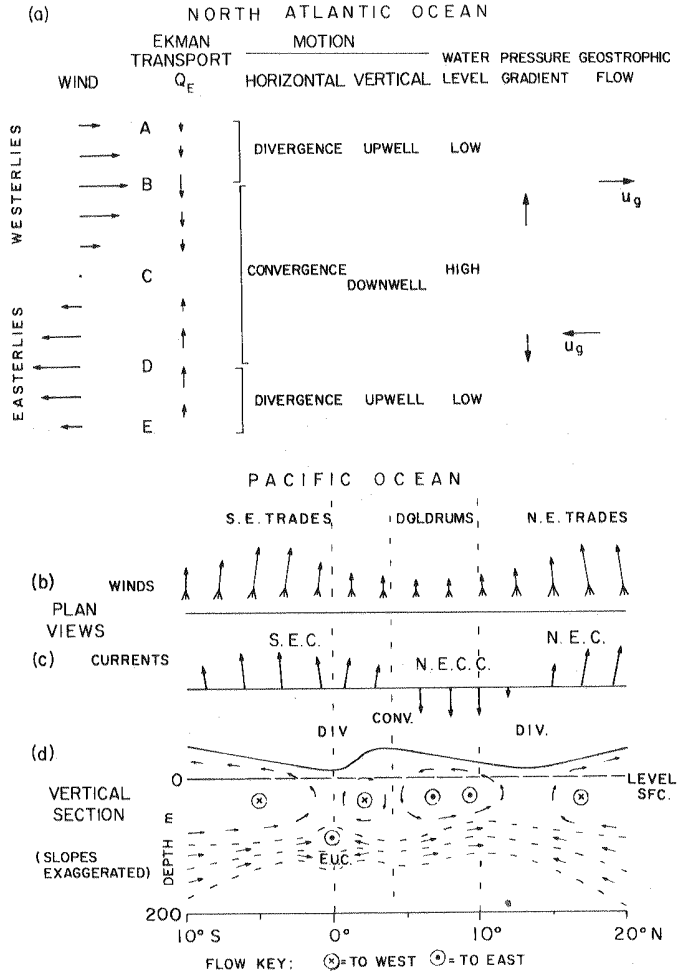

Fig. 9.6 (a) Convergences and divergences related to wind shear and associated geostrophic flow, North Atlantic Ocean; schematic representations in plan view for eastern equatorial Pacific Ocean of (b) wind system and (c) currents; (d) vertical section for same region showing circulation, convergences and divergences.

(1) The Ekman transport due to the wind will be in the southward direction from the westerlies and in the northward direction from the easterlies.

(2) The Ekman transport to the south will increase from A to B. To supply the increase, water must upwell from below the Ekman layer and there will be a zone of divergence.

(3) From B to C the southward Ekman flow will decrease to zero and from C to D it will be in a northward direction, increasing as one goes toward D. In consequence, the region around C will be one of convergence and water must descend below the surface.

(4) Between D and E there will be a region of divergence and upwelling.

(5) By setting up such pressure gradients the wind causes flows much deeper than those it drives directly in the Ekman layer. Thus the wind drives flows in the Ekman layer directly to 100 to 200 m depth, and geostrophic flows associated with convergence and divergence of the Ekman flows, and the pressure gradients which they cause, to depths of 1000 to 2000 m.

(6) In a region of convergence the surface level will tend to be ***high*** while in a divergence region it will tend to be ***low***, and there will be consequent pressure gradients and geostrophic flows (u_g) set up as shown on the right of Fig. 9.6(a).

(7) A wind blowing to the west along the equatorial zone (Fig. 9.6(b)), even without horizontal shear, will cause divergence and upwelling at the equator (Fig. 9.6(d)) because the Ekman layer transport will be to the right north of the equator and to the left south of the equator, i.e. away from the equator in both cases.

9.44 Bottom friction and shallow water effects

If a current is flowing over the sea bottom, friction there will generate an Ekman spiral current pattern above the sea bottom but with the direction of rotation of the spiral reversed relative to the wind-driven near-surface Ekman layer, i.e. anti- clockwise (Fig. 9.7).

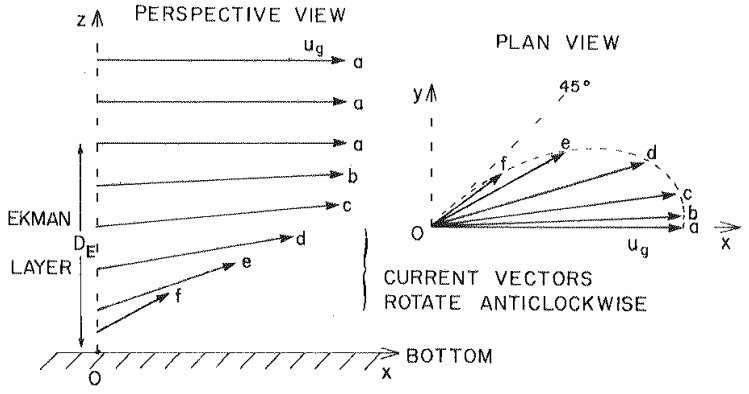

Fig. 9.7 Frictional effects on a geostrophic current near the bottom of the ocean (northern hemisphere).

Assuming

(1) A_z is constant

(2) The tangential velocity must vanish at the bottom (i.e. $u = v = 0$)

(3) The velocity goes to a constant value above the region of friction effects (the Ekman layer), assuming that the geostrophic flow above this layer is independent of z. $u = u_g$, $v = 0$ in the geostrophic region.

(4) The solution for the northern hemisphere is

$$\begin{aligned} u_E &= u_g\left[1-\exp(-\pi\, z/D_E)\cos(\pi\, z/D_E)\right] \\ v_E &= u_g \exp(-\pi\, z/D_E)\sin(\pi\, z/D_E) \end{aligned} \tag{9.17}$$

where z = 0 is taken at the bottom (see the derivative in class).

(5) At $z = 0$, $u_E = v_E = 0$. As z becomes large compared with D_E/π, $\exp(-\pi z/D_E)$ goes to zero and $u_E = u_g$, $v_E = 0$.

(6) Near the bottom u and v vary linearly with z and the near-bottom current direction is 45° to the left of the geostrophic current. The current rotates from the geostrophic direction to 45° to the left of it and the speed goes to zero at the bottom.

(7) The same solution is valid for wind blowing over the sea or land. Since in the northern hemisphere the surface wind is at 45° to the left of the geostrophic wind, i.e. the wind above the Ekman layer, and the surface (water) current at 45° to the right of the surface wind, the surface current will be in the same direction as the geostrophic wind.

(8) The direction of rotation to the left in the atmosphere is usually less than 45°, 10–20° is more commonly observed over the ocean. This discrepancy may be due to neglect of time-dependent and stability effects as well as to the simple form for A_z. Likewise, the wind-driven surface (water) current is likely to be to the right of the wind direction but not by exactly 45°.

(9) If the water becomes shallow and the depth decreases to order of D_E or less, the Ekman layer and the bottom Ekman layer will close up and overlap. In shallow water the two spirals tend to cancel each other so that the total transport is more in the direction of the surface wind rather than at right angles to it. When the water depth decreases to about $D_E/10$ then the transport is essentially in the wind direction, the effect of Coriolis force being swamped by the friction.

9.45 Limitation of the Ekman theory

Commenting on Ekman's assumptions:

(1) No boundaries — not realistic but probably not too bad an assumption away from the coast.

(2) Infinitely deep water — not exactly true but presents only a small source of error in the open ocean, i.e. D_E values of the order of 100 – 200 m compared with the average ocean depth of 4000 m.

(3) A_z constant — probably not true but at present we do not really know enough about it say whether or not this assumption leads to much error. It probably does not, because Rossby and Montgometry (1935) have solved the equations with $A_z = f(z)$ in likely ways and found only detailed differenced from Ekman's solution.

(4) Steady-state solution and steady wind — probably a real source of difficulty, since neither wind nor sea is really steady.

(5) There are other sources of motion in the sea and a current meter placed in the sea cannot distinguish one from another.

(6) Homogeneous water — distinctly unreal and one assumption that should be criticized although as noted the wind friction part of the flow can be calculated separately.

(7) The *f*–plane assumption — a minor source of error for zonal bodies of water and for areas of limited latitudinal extent.

9.5 Sverdrup's solution for the wind-driven circulation

Assuming negligible accelerations and friction from horizontal gradients of velocity

$$\begin{aligned} \alpha \frac{\partial p}{\partial x} &= f\, v + \alpha \frac{\partial \tau_x}{\partial z} \\ \alpha \frac{\partial p}{\partial y} &= -f\, u + \alpha \frac{\partial \tau_y}{\partial z} \end{aligned} \qquad (9.6')$$

i.e. Pessure = Coriolis + Friction (forces).

Sverdrup determined the total transport in the x and y directions in the whole layer affected by the wind (i.e. M_x and M_y when expressed as mass transport). He integrated the equations from the surface (taken as $z = 0$ because η will be small compared with the depth of frictional influence) to $z = -h$ (assumed to be above the ocean bottom) where the wind-driven motion has becomes zero. Such motion would include not only the Ekman but any geostrophic flows caused by divergence of the Ekman flow, so $h \gg D_E$. In the first stage of integration the equations take the form

$$\int_{-h}^{0} \frac{\partial p}{\partial x} dz = \int_{-h}^{0} \rho f v dz + \tau_{x\eta} = fM_y + \tau_{x\eta}$$
$$\int_{-h}^{0} \frac{\partial p}{\partial y} dz = -\int_{-h}^{0} \rho f u dz + \tau_{y\eta} = -fM_x + \tau_{y\eta} \qquad (9.18)$$

Here, $\tau_{x\eta}$ and $\tau_{y\eta}$ represent the wind-friction stress at the sea surface, all that remains of the friction terms in the previous pair of equation (9.6′). In this case the value of the friction stress in the water is equal to the wind stress at the surface $z = 0$ (the τ values), and is zero at $z = -h$.

From Equation (9.18), we can obtain

$$M_y \frac{\partial f}{\partial y} = \frac{\partial \tau_y}{\partial x} - \frac{\partial \tau_x}{\partial y} \qquad (9.19)$$

and together with the equation of continuity for mass transport

$$\frac{\partial M_y}{\partial y} + \frac{\partial M_x}{\partial x} = 0 \qquad (9.20)$$

Sverdrup's procedure assumes either that there is zero velocity in the deep water or that the bottom is level and that the friction there is small compared with that at the surface.

The interesting feature of (9.19) is that it is not the components themselves, τ_x and τ_y, of the wind surface stress $\vec{\tau}_\eta$ which appear but their horizontal ***gradients*** $\partial\tau_x/\partial y$ and $\partial\tau_y/\partial x$. Equation (9.19) becomes

$$\beta M_y = \mathrm{curl}_z\, \vec{\tau}_\eta \qquad (9.21)$$

where $\mathrm{curl}_z \vec{\tau}_\eta = \text{the vertical component of } \nabla \times \vec{\tau}_\eta = \frac{\partial \tau_y}{\partial x} - \frac{\partial \tau_x}{\partial y}$. Equation (9.21) is called the ***Sverdrup equation***.

We can write that M_x (total) = M_{xE} (Ekman) + M_{xg} (geostrophic). The equation (9.18) becomes

$$fM_{yE} = f\int_{-h}^{0} \rho v_E dz = -\tau_x$$
$$fM_{yg} = f\int_{-h}^{0} \rho v_g dz = \int_{-h}^{0} \frac{\partial p}{\partial x} dz \qquad (9.22)$$

and similarly for M_x.

9.51 Orders of magnitude of the terms

For example, we use a position in the North Atlantic at about 35°N with a wind of 7–8 ms^{-1} from the west. Then $\tau_x \cong 10^{-1}$ Nm^{-2} and $\tau_y = 0$,

$$\text{curl}_z\ \vec{\tau}_\eta \cong -\frac{\partial \tau_x}{\partial y} \cong -\frac{10^{-1}\ \text{Nm}^{-2}}{1000\,\text{km}} \cong -10^{-7}\ \text{Nm}^{-3}$$

$$f \cong 10^{-4}\ \text{s}^{-1}, \quad \beta \cong 2\times 10^{-11}\ \text{m}^{-1}\text{s}^{-1}$$

Using (9.16) we get

$$M_{yE} = -\frac{\tau_x}{f} = -10^3\ \text{kg m}^{-1}\text{s}^{-1}$$

and using (9.21)

$$M_y = M_{yE} + M_{yg} = \frac{\text{curl}_z\ \vec{\tau}_\eta}{\beta} = -\frac{10^{-7}}{2\times 10^{-11}} = -5\times 10^3\ \text{kg m}^{-1}\text{s}^{-1}$$

We see that $M_{yg} = -4\times 10^3$ kg m^{-1}s^{-1} which is caused by the north-south variation of the wind and consequent convergence of M_{yE} and is considerably larger than M_{yE} as is often the case.

The value for M_y above is for only a 1-m-wide strip, so that for the width of an ocean of 5000 km = 5×10^6 m, the southward flow would be 25×10^9 kg s^{-1} $\cong 25 \times 10^6$ m^{3}s^{-1} in volume = 25 Sverdrups.

9.52 Application of the Sverdrup equations

Sverdrup applied these equations to the trade-wind zones in lower latitudes where τ_y and $\partial \tau_y/\partial x$ can be assumed to be negligible. Note that $f = 2\Omega \sin \phi$, $dy = R\, d\phi$, and $\beta = df/dy = 2\Omega \cos\phi/R$. Using (9.20)

$$\frac{\partial M_x}{\partial x} = -\frac{\partial M_y}{\partial y} = \frac{1}{2\Omega\cos\phi}\left(R\frac{\partial^2 \bar{\tau}_x}{\partial y^2} + \frac{\partial \bar{\tau}_x}{\partial y}\tan\phi\right)$$

Note:

$$\frac{\partial M_x}{\partial x} = -\frac{\partial M_y}{\partial y} = \frac{\partial}{\partial y}\left[\frac{R}{2\Omega\cos\phi}\frac{\partial \tau_x}{\partial y}\right] = \frac{R}{2\Omega\cos\phi}\frac{\partial^2 \tau_x}{\partial y^2} + \frac{\partial \tau_x}{\partial y}\frac{\partial}{\partial y}\left[\frac{R}{2\Omega\cos\phi}\right]$$

$$= \frac{R}{2\Omega\cos\phi}\frac{\partial^2 \tau_x}{\partial y^2} + R\frac{\partial \sec\phi}{\partial \phi}\frac{\partial \tau_x}{\partial y} = \frac{1}{2\Omega\cos\phi}\left[R\frac{\partial^2 \tau_x}{\partial y^2} + \frac{\partial \tau_x}{\partial y}\tan\phi\right]$$

since $\dfrac{\partial \sec\phi}{\partial \phi} = \sec\phi\tan\phi$.

---

which can be integrated from $x = 0$, the coast, where $M_x = 0$. Finally, we have

$$M_x = \frac{x}{2\Omega\cos\phi}\left(\frac{\partial\bar{\tau}_x}{\partial y}\tan\phi + \frac{\partial^2\bar{\tau}_x}{\partial y^2}R\right),$$
$$M_y = -\frac{R}{2\Omega\cos\phi}\frac{\partial\bar{\tau}_x}{\partial y} \qquad (9.23)$$

Here x is the distance from a north-south coastline at the east side of the ocean westward to a point **P** in the ocean as in Fig. 9.8.

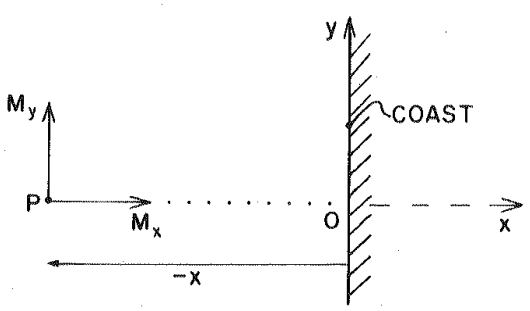

Fig. 9.8 For derivation of the Sverdrup transport on the east side of an ocean.

Note:

(a) $\int_0^x dM_x = \int_0^x \frac{1}{2\Omega\cos\phi}\left[R\frac{\partial^2\tau_x}{\partial y^2} + \frac{\partial\tau_x}{\partial y}\tan\phi\right]dx$

$$M_x = \frac{x}{2\Omega\cos\phi}\left[R\frac{\partial^2\tau_x}{\partial y^2} + \frac{\partial\tau_x}{\partial y}\tan\phi\right]$$

(b) $\int_0^y dM_y = -\int_0^y \frac{1}{2\Omega\cos\phi}\left[R\frac{\partial^2\tau_x}{\partial y^2} + \frac{\partial\tau_x}{\partial y}\tan\phi\right]dy$

$$M_y = -\int_0^y \frac{1}{2\Omega\cos\phi}\left[R\frac{\partial^2\tau_x}{\partial y^2} + \frac{\partial\tau_x}{\partial y}\tan\phi\right]Rd\phi$$
$$= -\int_0^y \frac{1}{2\Omega\cos\phi}R^2\frac{\partial^2\tau_x}{\partial y^2}d\phi - \int_0^y \frac{\partial\tau_x}{\partial y}\frac{R\tan\phi}{2\Omega\cos\phi}d\phi \qquad \text{(b-1)}$$
$$= -\frac{R^2}{2\Omega}\frac{\partial^2\tau_x}{\partial y^2}\ln\tan\left(\frac{\phi}{2} + \frac{\pi}{4}\right) - \frac{R}{2\Omega\cos\phi}\frac{\partial\tau_x}{\partial y}$$

formulas:

(1) $\int \sec^n ax\tan axdx = \frac{\sec^n ax}{na}$

(2) $\int \sec axdx = \frac{1}{a}\ln(\sec ax + \tan ax) = \frac{1}{a}\ln\tan(\frac{ax}{2} + \frac{\pi}{4})$

The first term of the right-hand side in (b-1) can be negligible.

Comparing the Ekman and the Sverdrup solutions:

(1) Sverdrup lost the details of the current velocities with depth but gained the possibility of having a coastal boundary at one side of the ocean, a step toward a more realistic situation than Ekman's horizontally infinite, i.e. boundaryless, ocean.

(2) Sverdrup's solution also is no longer bound by the homogeneous ocean assumption and the solutions therefore have this additional feature of the real oceans.

Eq. (9.23), it turns out in practical that in the trade wind and equatorial (tropical) zones $R\frac{\partial^2 \tau_x}{\partial y^2} >> \tan\phi \frac{\partial \tau_x}{\partial y}$

So, $M_x = \frac{x}{\beta}\frac{\partial^2 \tau_x}{\partial y^2}$, $M_y = -\frac{1}{\beta}\frac{\partial \tau_x}{\partial y}$

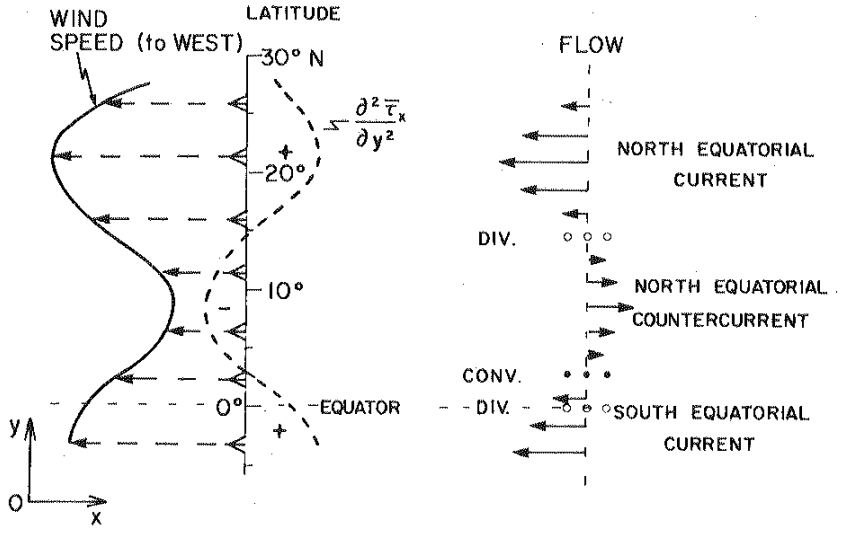

Fig. 9.9 Smoothed representation of the east–west components of wind speed and stress terms, and related currents at low latitudes, eastern Pacific Ocean. Regions of divergence (DIV) and convergence (CONV) indicated.

Fig. 9.9 shows for the eastern Pacific the character of the mean *x*-component of the wind as the full line while the corresponding character of $\partial^2 \bar{\tau}_x / \partial y^2$ is shown by the dashed line.

(a) north of about 15°N and south of about 2°N, the value of $\partial^2\bar{\tau}_x/\partial y^2$ is + and x is –, $\therefore$ M_x is –, i.e. the flow is to the **west** (North Equatorial Current and South Equatorial Current)

(b) between 15°N and 2°N (the doldrums), the value $\partial^2\bar{\tau}_x/\partial y^2$ is – and x is –, $\therefore M_x$ is +, i.e. the flow is to the east (North Equatorial Countercurrent).

(c) This figure shows qualitatively how Sverdrup's solution explains the existence of an equatorial current system consisting of two westward flowing currents (NEC and SEC) with an eastward flowing current (NECC) between them.

(d) Note that this system is not symmetrical about the equator but is displaced to the north of it, because the trade-wind system is displaced this way in the Pacific.

(e) The current distribution is similar in the Atlantic.

(f) In the Indian Ocean, the wind pattern changes seasonally and the current pattern changes with it.

(1) During the Northeast Monsoon (Nov. to March), the wind pattern is similar to those in the Pacific and Atlantic but is situated somewhat further south; the westward NEC straddles the equator and the eastward Equatorial Countercurrent and the SEC are both south of the equator.

(2) During the Southwest Monsoon (May to Sept.), the Southeast Trade Winds continue south of the equator but north of the equator the winds blow to the northeast (called the Southwest Monsoon). As a result there is only a two-current system – the wind-driven Southwest Monsoon Current to the east straddling the equator and SEC to the west well south of the equator.

(g) The equatorial current system is now known to be more complicated than shown by the Sverdrup theory.

Sverdrup went on to test the solutions quantitatively by:

(a) calculating τ_x from the known mean winds and then calculating the curl, etc., and thence the values for M_x and M_y at selected positions defined by x (the distance from the eastern boundary),

(b) determining M_{xg} and M_{yg} independently by the geostrophic method from oceanographic field data and adding the Ekman transport to get the total transport,

(c) comparing these two independent calculations.

Fig. 9.10 shows the result of this calculation as revised by Reid (1948).

Note that $M_x \cong 10M_y$ which is fairly typical, particularly for equatorial regions. The reason lies in the difference between the east–west and the north–south length scales of the gyre systems. The east–west scale (L_x) is determined by continental barriers, the north–south (L_y) by the lines of $\text{curl}_z\, \vec{\tau}_\eta = 0$. Typically $L_x/L_y \cong 10$. By continuity

$$\frac{\partial M_x}{\partial x} + \frac{\partial M_y}{\partial y} = 0, \quad \text{then} \frac{M_x}{M_y} \cong \frac{L_x}{L_y} \cong \frac{10}{1}$$

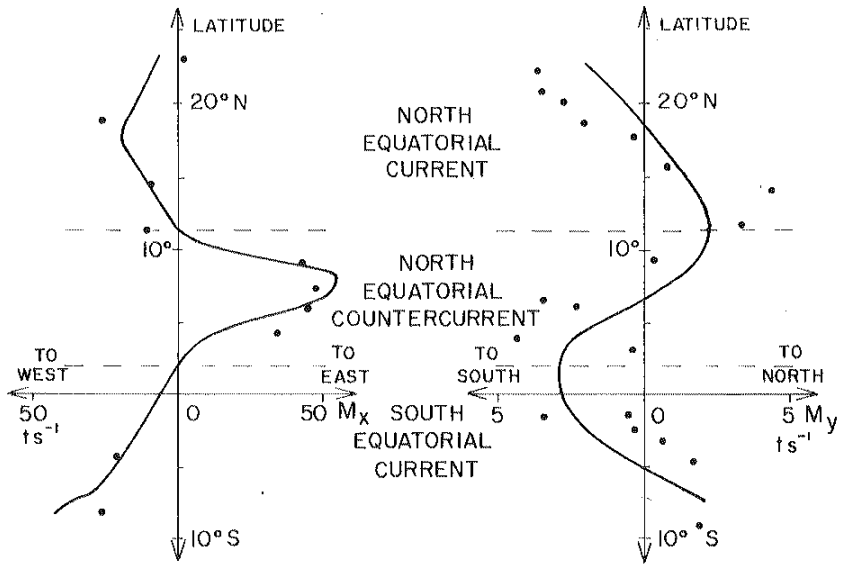

Fig. 9.10 Mass transport components in the eastern Pacific calculated from the mean wind stress (lines) compared to those from geostrophic calculations from oceanographic data (dots). M_x and M_y in tons per second through a vertical data 1 m wide and 1000 m deep (approximately) equivalent to 0.1 Sv per degree of latitude). (From Reid, 1948.)

Fig. 9.11 shows an analytic solution by R.O. Reid (1948) calculated from a simplified form for the wind stress but for the real coastline in the eastern equatorial Pacific.

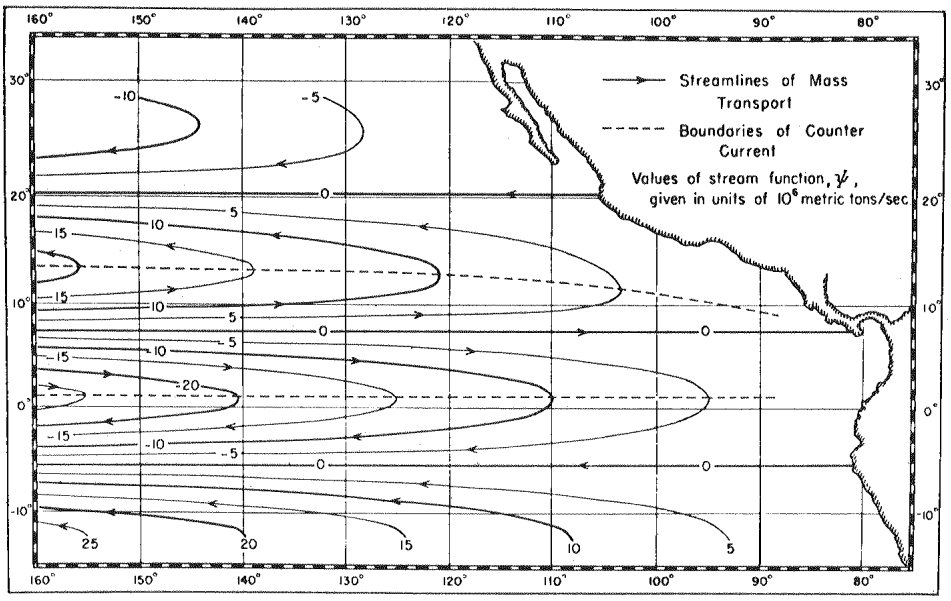

Fig. 9.11 Streamlines of mass transport in the eastern Pacific from the mean wind stress (From Reid, 1948).

Limitations of the Sverdrup theory:

(1) It is limited in application to the neighborhood of the east side of the ocean, because the x in the expression for M_x would increase in direct proportion to the distance to the west. M_x does increase somewhat to the west but not as fast as the expression would suggest. Probably the reason for this discrepancy is that lateral friction (between the currents) has been ignored.

(2) The differential equations allow only one boundary condition to be satisfied; in the solution given it is that there shall be no flow through the coast. To be able to apply more boundary conditions (e.g. no slip at the eastern boundary and perhaps conditions at a western boundary) it is necessary to go to more complicated equations.

(3) The solutions give the depth integrated mass transport but no details of the velocity distribution with depth.

9.6 The general form of the Sverdrup equation – convergence and divergence

Consider a column of fluid with sides δx and δy extending from the sea surface to $z = -h$. Mass transports in the x and y directions respectively are

$$M_x = \int_{-h}^{\eta} \rho\, u\, dz \quad \text{and} \quad M_y = \int_{-h}^{\eta} \rho\, v\, dz$$

(1) The mass flow into the column in the x-direction is $M_x \delta y$ and the flow out is $[M_x + (\partial M_x/\partial x)\delta x]\delta y$. The net flow out in the x-direction is $(\partial M_x/\partial x)\delta x \delta y$.

Similarly in the *y*-direction it is $(\partial M_y/\partial y)\delta x\delta y$.

(2) At the bottom of the column ($z = -h$) there may be flow out if the vertical velocity is not zero; it will be $-\rho w_{-h}\delta x\delta y$.

(3) At the top there may be an effective outflow velocity w_η if there is a net difference between evaporation and precipitation. We shall neglect this effect but it could be included as a driving term.

(4) Because mass must be conserved, the net flow of mass out must be zero, i.e.

$$\left(\frac{\partial M_x}{\partial x}+\frac{\partial M_y}{\partial y}-\rho\, w_{-h}\right)\delta x\delta y=0$$

So, it can be written as

$$\frac{\partial M_x}{\partial x}+\frac{\partial M_y}{\partial y}-\rho\, w_{-h}=0$$

or

$$\nabla_H\cdot\vec{M}-\rho\, w_{-h}=0 \qquad (9.24)$$

(5) If the velocity is zero at $z = -h$ and deeper, then $w_{-h}=0$ and we get the form used by Sverdrup. If $h = -z_B$ is the total depth the last term of Eq. (9.24) also vanishes because there can be no through the bottom.

(6) It is convenient to take the point of view that the vertical velocity associated with the divergence of one type of transport provides a driving force for the convergence of another type of transport.

For example, consider the Ekman flow, then $\dfrac{\partial M_{xE}}{\partial x}+\dfrac{\partial M_{yE}}{\partial y}-\rho\, w_E=0.$

Here w_E is the vertical velocity at the bottom of the Ekman layer associated with convergence or divergence of the Ekman transport.
If $w_E \neq 0$, it requires a corresponding divergence or convergence of flow below.

(7) Assume that the flow vanishes below $z = -h$, so that $w_{-h} = 0$, then $\nabla_H\cdot\vec{M}=\nabla_H\cdot\left(\vec{M}_E+\vec{M}_g\right)=0.$ Thus, $\nabla_H\cdot\vec{M}_g=-\nabla_H\cdot\vec{M}_E=-\rho\, w_E$. The process sometimes spoken of as ***Ekman pumping***.

(8) If the flow does not go to zero before approaching the bottom, there may be a bottom Ekman layer. Then $\nabla_H\cdot\vec{M}_{EB}+\rho\, w_{EB}=0$ where ρw_{EB} is added

since it is flow up through the top and $\nabla_H \cdot \vec{M}_g = -\rho(w_E - w_{EB})$.

(9) We expect w_{EB} to be rather small compared with w_E as a general rule. Note that w_E is a good approximation to the total vertical velocity at the base of the layer.

(10) The volume transports, $Q_x = \int_{-h}^{\eta} u dz$ and $Q_y = \int_{-h}^{\eta} v dz$. So,

$$\frac{\partial Q_x}{\partial x} + \frac{\partial Q_y}{\partial y} - w_{-h} = 0 \tag{9.25}$$

In (9.6) accelerations and friction from velocity variations in the horizontal have been assumed small; this should be a good approximation except in strong currents such as the Gulf Stream. We obtain

$$\begin{aligned} \int_{z_B}^{\eta} \frac{\partial p}{\partial x} dz &= fM_y + \tau_{x\eta} - \tau_{xB} \\ \int_{z_B}^{\eta} \frac{\partial p}{\partial y} dz &= -fM_x + \tau_{y\eta} - \tau_{yB} \end{aligned} \tag{9.26}$$

(11)Define a function

$E_P = \int_{z_B}^{\eta} \rho g(z - z_B) dz$ = work done to pile up the water above the bottom, i.e. it is a measure of the potential energy. Now

$E_p = \frac{1}{g} \int_{z_B}^{\eta} (p\alpha) \rho g dz$ is the origin definition rewritten.

Using the hydrostatic equation $dp = -\rho g dz$ and $p = 0$ at $z = \eta$, $p = p_B$ at $z = z_B$. We have

$$E_p = \frac{1}{g} \int_0^{p_B} p\alpha dp = \frac{1}{g} \int_0^{p_B} p\alpha_0 dp + \frac{1}{g} \int_0^{p_B} p\delta dp = E_p^0 + \chi \tag{9.27}$$

E_p^0 is a function of the bottom pressure only; it is equal to the potential energy of sea water S_o=35, T=0°C. χ is the potential energy anomaly, i.e. the difference from E_p^0 associated with the difference between the reference specific volume and the actual specific volume.

$$\frac{\partial}{\partial x} \int_{z_B}^{\eta} p dz = \int_{z_B}^{\eta} \frac{\partial p}{\partial x} dz + p_\eta \frac{\partial \eta}{\partial x} - p_B \frac{\partial z_B}{\partial x}$$

We take $p_\eta = 0$, rearrange

$$\int_{z_B}^{\eta} \frac{\partial p}{\partial x} dz = \frac{\partial E_p}{\partial x} + p_B \frac{\partial z_B}{\partial x} = \frac{\partial \chi}{\partial x} + \frac{\partial E_p^0}{\partial x} + p_B \frac{\partial z_B}{\partial x} \tag{9.28}$$

The last two terms may be combined (see Fofonoff, 1962) to give

$$\int_{z_B}^{\eta} \frac{\partial p}{\partial x} dz = \frac{\partial \chi}{\partial x} + \frac{p_B \alpha_B}{g} \left(\frac{\partial p_B}{\partial x} \right)_z \tag{9.29}$$

where $(\partial p_B/\partial x)_z$ means the change of pressure on a level surface at the bottom. The *y*-component equation can also be obtained. From (9.26)

$$\begin{aligned} -fM_y &= -\frac{\partial \chi}{\partial x} - \frac{p_B \alpha_B}{g} \left(\frac{\partial p_B}{\partial x} \right)_z + \tau_{x\eta} - \tau_{xB} \\ fM_x &= -\frac{\partial \chi}{\partial y} - \frac{p_B \alpha_B}{g} \left(\frac{\partial p_B}{\partial y} \right)_z + \tau_{y\eta} - \tau_{yB} \end{aligned} \tag{9.30}$$

(a) The first terms are associated with variations in the density distribution; they arise from the ***baroclinic*** part of the geostrophic velocity, i.e.

$$f\, M_{yc} = \frac{\partial \chi}{\partial x}, \quad f\, M_{xc} = -\frac{\partial \chi}{\partial y}$$

(b) The stress terms may be associated with Ekman transports

$$f\, M_{yE} = -\tau_{x\eta}\,; \quad f\, M_{yEB} = \tau_{xB}\,; \quad f\, M_{xE} = \tau_{y\eta}\,; \quad f\, M_{xEB} = -\tau_{yB}$$

(c) The terms involving bottom pressure are the ***barotropic*** transport times *f*. $M_{yb} = \int_{z_B}^{\eta} \rho\, v_b dz = v_b \int_{z_B}^{\eta} \rho\, dz$.

Now $\rho\, dz = -\frac{dp}{g}$, so $\int_{z_B}^{\eta} \rho\, dz = -\int_{p_B}^{\eta} \frac{dp}{g} = \frac{p_B}{g}$, and $M_{yb} = \frac{v_b p_B}{g}$.

The barotropic flow is the geostrophic flow in the deep water, so

$$f\, v_b = \alpha_B \left(\frac{\partial p_B}{\partial x} \right)_z \quad \text{and} \quad \frac{p_B \alpha_B}{g} \left(\frac{\partial p_B}{\partial x} \right)_z = \frac{f\, v_b p_B}{g} = f\, M_{yb}$$

Likewise, the p_B term in the second equation of (9.30) is $-fM_{xb}$. Thus equation (9.30) may be written as

$$\begin{aligned} M_y &= M_{yc} + M_{yb} + M_{yE} + M_{yEB} \\ M_x &= M_{xc} + M_{xb} + M_{xE} + M_{xEB} \end{aligned} \tag{9.30'}$$

These equations simply divide the total transport into components, which are related respectively to the density field, bottom pressure gradient and stress

terms of equation (9.30).

Now, following Sverdrup's approach we take

$$\frac{\partial}{\partial x}\left(fM_x\right)+\frac{\partial}{\partial y}\left(fM_y\right)=f\left(\frac{\partial M_x}{\partial x}+\frac{\partial M_y}{\partial y}\right)+\beta M_y=\beta M_y \qquad (9.31)$$

because by continuity $(\partial M_x/\partial x+\partial M_y/\partial y)=0$ for the total transport from surface to bottom. Thus (9.30) can be written as

$$\beta M_y=\mathrm{curl}_z\,\vec{\tau}_\eta-\mathrm{curl}_z\,\vec{\tau}_B-\rho'\,f\left(u_b\frac{\partial z_B}{\partial x}+v_b\frac{\partial z_B}{\partial y}\right) \qquad (9.32)$$

or in vector form

$$\beta M_y=\left(\nabla\times\vec{\tau}_\eta\right)_k-\left(\nabla\times\vec{\tau}_B\right)_k-\rho'\,f\left(\vec{V}_b\cdot\nabla_H\,z_B\right)$$

where $\nabla_H=\vec{i}\left(\frac{\partial}{\partial x}\right)+\vec{j}\left(\frac{\partial}{\partial y}\right)$ and $\rho'=\rho_B\left[1+\frac{p_B}{\alpha_B}\left(\frac{\partial\alpha}{\partial p}\right)_B\right]$

Note that the following three assumptions make (9.32) reduced to the simpler form of (9.21) derived by Sverdrup.

(1) Sverdrup assumed the deep flow (barotropic part) to be zero. With no flow near the bottom there is no stress there either.

(2) If the bottom is level and the bottom stress negligible.

(3) If the flow is along the bottom contours, i.e. is entirely horizontal so that $\vec{V}_b$ is perpendicular to $\nabla_H z_B$, then the terms involving z_B also vanish. It has been quite common to neglect the bottom stress.

9.7 The mass transport stream function

By integrating along the vertical, we have derived the mass transport per unit width of current which depends on *x* and *y* but not on *z*. When we have such a flow, it is possible to use a scalar function called a ***stream function*** from which the velocity may be derived.

$$M_x=\frac{\partial\psi}{\partial y}\qquad M_y=-\frac{\partial\psi}{\partial x} \qquad (9.33)$$

where ψ is the stream function. The flow is parallel to lines on which ψ is a constant, which means that plots showing such lines are convenient for display purposes as shown in Fig. 9.11.

While the total transport is non-divergent, i.e. continuity takes the form

$$\frac{\partial M_x}{\partial x} + \frac{\partial M_y}{\partial y} = \nabla_H \cdot \vec{M} = 0$$

(1) The individual transports, Ekman, baroclinic, barotropic (if any) and bottom Ekman (if any) may not be so; it may not be possible to represent them by stream functions.

(2) The negative of the potential energy anomaly ($-\chi$) is almost a stream function for the baroclinic transport.

(3) Actually, contours of ($-\chi$) are "streamlines" for fM_c but since f varies slowly the baroclinic flow will be almost along the contours. The relation between the contour spacing and the strength of the transport will vary with f and hence with latitude.

(4) Similarly, a contour plot of $\Delta\Phi$ (or ΔD) shows the pattern of the horizontal geostrophic flow (relative to that at the reference level). It is not a true stream function unless $(\partial u/\partial x)+(\partial v/\partial y)=0$ is also true, but it provides the same useful display features as a stream function.

9.8 Westward intensification — Stommel's contribution

Stommel (1948) was the first to present an adequate explanation for the ***westward intensification***. His demonstration was done with a simplified theoretical model of an ocean and wind pattern; (1) flat bottom and (2) a wind stress which varies with latitude as shown in Fig. 9.12. He calculated the flow patterns for three conditions:

(1) non-rotating ocean (i.e. non-rotating earth);

(2) rotating ocean but Coriolis parameter f constant (the f-plane approximation);

(3) rotating earth with Coriolis parameter varying with latitude ϕ in a simple but realistic fashion, i.e. linearly with latitude ϕ from 10° to 50° latitude (the β-plane approximation).

Fig. 9.12(b) is most like the flow pattern in the real oceans. In case (1) the surface remained nearly level. In case (2), to balance the ***Coriolis*** effect a higher water level was found at the center to provide the necessary pressure gradient (fig. 9.12(a)). A similar high level was found in case (3) but it was not symmetric in the east-west direction as in case (2) but displaced to the west (Fig. 9.12(b)).

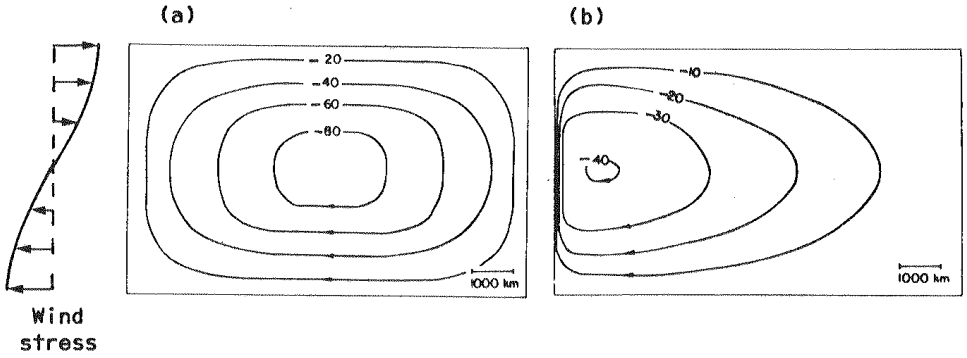

Fig. 9.12 Flow patterns (streamlines) for simplified wind-driven circulation with: (a) Coriolis force zero or constant, (b) Coriolis force increasing linearly with latitude. (From Stommel, 1948).

The variation with latitude, $\partial f/\partial \phi$, of the Coriolis parameter was responsible for the westward intensification. Nowadays, this result is discussed in terms of vorticity. We will discuss it later.

(1) The result of Stommel's was obtained for a very simplified version of the real ocean, but it is clear that the variation of the Coriolis parameter is a fundamental feature of the dynamics, which must be taken into account in any study of large ocean circulations.

(2) Stommel's addition of a friction term permitted a solution with a closed circulation, which Sverdrup's assumptions did not.

(3) For a fuller exposition, you can consult Stommel's book "The *Gulf Stream* (1965)."

9.9 The planetary wind field and the drag coefficient C_D

The main features of the general pattern of the global winds are shown in Fig. 9.13.

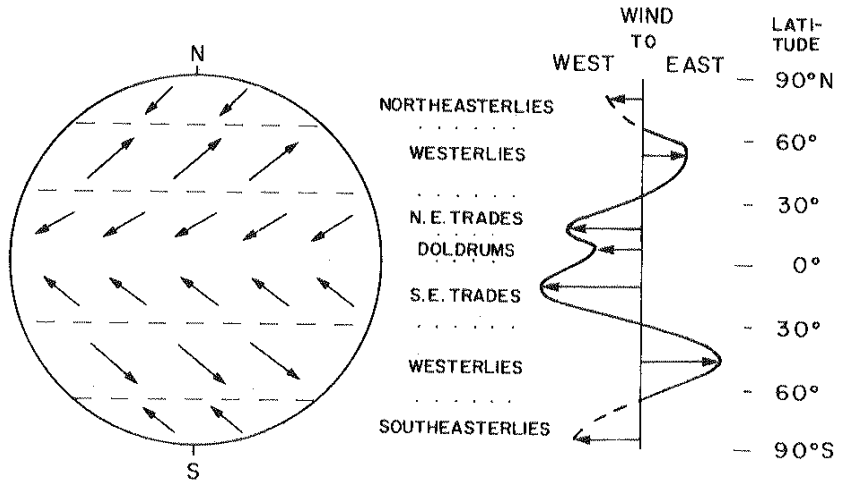

Fig. 9.13 General pattern of global winds and mean east–west wind components.

The graph of the east-west component of the wind on the right shows that Stommel's form for the wind stress, as a function of latitude, is a reasonable approximation to the real stress between about 10° and 50°N.

The procedure is to use the relation that wind stress $\tau = \rho\, C_D\, W^2$ in the direction of the wind W. The problem is what value to use for the drag coefficient C_D. As far as we know, most stress calculation for oceanographic purposes have used a step or smoothed step function for C_D as in Fig. 9.14 (Smith, 1980; Large and Pond, 1981). Note that C_D is a function of height since wind speed varies with height. The values shown are for a measurement height of 10 m above sea level.

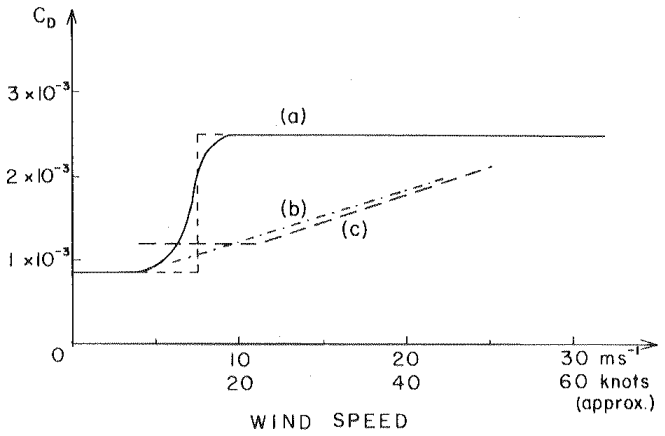

Fig. 9.14 Form of drag coefficient (C_D) for wind over water as a function of wind speed: (a) as used for many calculations of wind- driven circulation; measured values for 10 m height for neutral stability by (b) Smith (1980), (c) Large and Pond (1981).

9.10 Munk's solution

Munk combined the basic features contributed by Ekman, Sverdrup and Stommel to provide the first comprehensive solution for the wind-driven circulation, using the real wind field, albeit with less detailed wind roses than are now available and using the step function C_D. He used two friction terms:

(1) vertical, associated with vertical shear to convey momentum from the wind stress applied at the surface into the Ekman layer,

(2) lateral, associated with horizontal shear so that the ocean would remain in a steady state of circulation.

He finished up with a 4th-order differential equation describing the circulation as

$$A\nabla^4\psi - \left(\beta\frac{\partial\psi}{\partial x}\right) - \text{curl}_z\ \vec{\tau}_\eta = 0 \qquad (9.34)$$

where A = the eddy viscosity coefficient for lateral friction for mass transport.

∇^4 = the 2D bi-harmonic operator = $\dfrac{\partial^4}{\partial x^4} + 2\dfrac{\partial^4}{\partial x^2\partial y^2} + \dfrac{\partial^4}{\partial y^4}$

ψ = the mass transport stream function which describes the stream lines (really trajectories in the steady state) of flow around the ocean.

The equation must be solved for ψ and then

$$M_x = \frac{\partial\psi}{\partial y}, \qquad M_y = -\frac{\partial\psi}{\partial x}$$

In words, Eq. (9.34) can be written

Vorticity from lateral stress – ***Planetary vorticity*** – ***Wind stress curl*** = 0

The three terms in the equation are not equally important all over the ocean.

(1) In the west, where the currents are strong, the first and second are the important ones; (the lateral stress is determined by the lateral shear in the currents and is large in the west because the currents and shear are large there.)

(2) In the remainder of the ocean the second and third are important.

(3) Munk used values for the east-west wind stress component. For the solution, ψ is shown in Fig. 9.15(a). This is the solution for a rectangular ocean and is somewhat stylized.

(4) Later, Munk and Carrier solved a triangular ocean, which is more nearly represents the real shape of the North Pacific as shown in Fig. 9.15(b).

Note that the second and third terms are just the Sverdrup equation (9.21) with $-\partial\psi/\partial x$ substituted for M_y.

Munk assumed

(1) The currents went to zero above the bottom or the bottom was a level and the bottom stress was negligible because the currents ought to be very small in the deep water.

(2) In the west, the friction terms associated with horizontal shears in the

currents would become important but that non-linear terms would remain small.

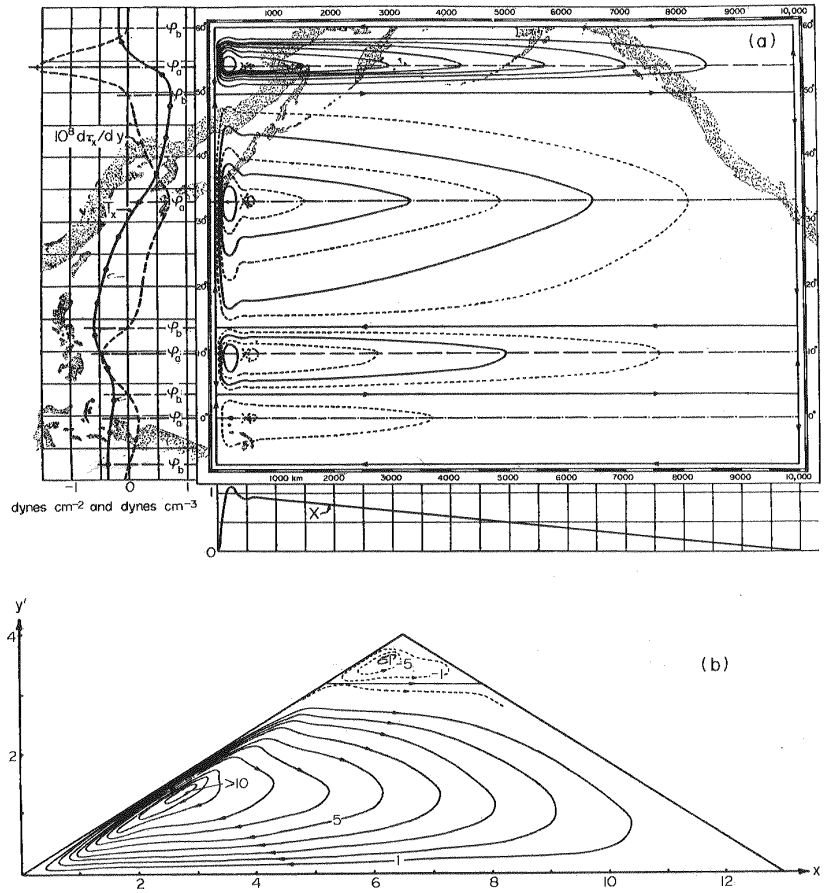

Fig. 9.15 (a) on left – mean annual wind stress over the Pacific, τ_x (full line) and its curl, $10^8\ \partial\tau_x/\partial y$ (dashed line), on right – computed mass transport streamlines (ψ) for a rectangular ocean (from Munk, 1950); (b) computed transport streamlines for a triangular ocean from 15° to 60°N (from Munk and Carrier, 1950). (1 dyne cm^{-2} = 0.1 Pa; 1 dyne cm^{-3} = 10 Pa m^{-1}.)

How Munk's equation (9.34) is obtained, we start from the vertically integrated equation (9.30) but add the lateral friction terms. For simplicity we omit the bottom pressure and stress terms as Munk's assumptions

$$-f M_y = -\frac{\partial \chi}{\partial x} + \tau_{x\eta} + \int_{z_B}^{\eta} \rho A_x \frac{\partial^2 u}{\partial x^2} dz + \int_{z_B}^{\eta} \rho A_y \frac{\partial^2 u}{\partial y^2} dz$$

$$f M_x = -\frac{\partial \chi}{\partial y} + \tau_{y\eta} + \int_{z_B}^{\eta} \rho A_x \frac{\partial^2 v}{\partial x^2} dz + \int_{z_B}^{\eta} \rho A_y \frac{\partial^2 v}{\partial y^2} dz$$

Now assume that $A_x = A_y = A_H$ and that

$$\int_{z_B}^{\eta} \rho A_H \frac{\partial^2 u}{\partial x^2} dz \cong A \frac{\partial^2 M_x}{\partial x^2}$$

Assume the eddy viscosity, A, is constant. Using $M_x = \partial\psi/\partial y$, $M_y = -\partial\psi/\partial x$, we

have

$$-A\left[\frac{\partial}{\partial x}\left(\frac{\partial^2}{\partial x^2}+\frac{\partial^2}{\partial y^2}\right)\frac{\partial \psi}{\partial x}+\frac{\partial}{\partial y}\left(\frac{\partial^2}{\partial x^2}+\frac{\partial^2}{\partial y^2}\right)\frac{\partial \psi}{\partial y}\right]$$
$$=-A\left[\frac{\partial^4 \psi}{\partial x^4}+2\frac{\partial^4 \psi}{\partial x^2 \partial y^2}+\frac{\partial^4 \psi}{\partial y^4}\right]=-A\nabla^4\psi$$

and we have finally

$$\boxed{\beta M_y=-\beta\frac{\partial \psi}{\partial x}=\text{curl}_z\,\vec{\tau}_\eta-A\nabla^4\psi}$$

which is Munk's equation.

Note that

(1) This is a 4th-order equation and therefore its solution can satisfy 4 boundary conditions — no flow through and no-slip along both east and west boundaries.

(2) The vanishing of $\text{curl}_z\,\vec{\tau}_\eta$ at certain latitudes breaks the flow into gyres as in Fig. 9.15.

(3) In Stommel's model, because of the simpler form in which he assumed for the friction term, his equation was only of second order and he could not satisfy the no-slip condition.

(4) Because of higher order, Munk's solution allows for the counter- current (a fairly strong southward flow observed to the east of the Kuroshio and the Gulf Stream).

(5) In Fig. 9.15, the western boundary current is where the streamlines are close together indicating strong currents.

(6) The countercurrent is indicated in the largest gyre by the swing to the south of the streamlines as they enter and leave this region.

(7) Stommel's model (Fig. 9.12(b)) does show the western intensification but not the countercurrent. Munk's solution is more realistic in these regards.

Comments on Munk's solution:

(1) Munk's calculated transport was about ½ the accepted value based on measurements of the Gulf Stream.

(2) Recent recalculations show good agreement except for the region offshore of Cape Hatteras where there is a strong recirculation.

(3) Munk's solution was based on wind stress averages over 5°squares. This underestimates the curl of the stress. 1° averages are difficult to obtain, but they are starting to become available.

(4) Leema and Bunker (1978) used modern drag coefficient and 2°×5° averages of stress to obtain 32 Sv transport in the Gulf Stream.

9.11 Vorticity

9.11.1 *Relative vorticity*—ζ

Vorticity is a characteristic of the kinematics of fluid flow, which expresses the tendency for portions of the fluid to rotate. It is directly associated with the quantity called "velocity shear" as illustrated in Fig. 9.16(a).

(1) When it is measured relative to the earth it is called ***relative vorticity*** (ζ).

(2) When it is measured relative to axes fixed in space it is called "absolute vorticity".

(3) The vorticity is positive when it is anticlockwise.

(4) The relative vorticity in the horizontal plane (the vertical component) is

$$\zeta = \text{curl}_z \vec{V} = \left(\partial v/\partial x - \partial u/\partial y\right).$$

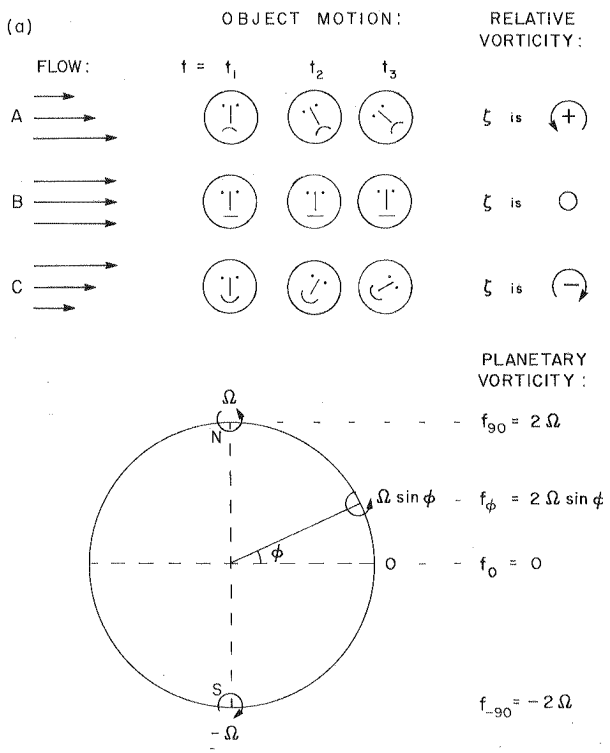

Fig. 9.16 For discussion of vorticity: (a) relation between relative vorticity (ζ) and velocity shear, (b) planetary vorticity (f) at various latitudes on a rotating earth.

9.11.2 *Planetary vorticity—f*

For a rotating solid object, the vorticity = 2 × angular velocity. By the virtue of the rotation of the earth in space, at the latitude ϕ a portion of its surface has angular velocity $\Omega\sin\phi$ about a vertical axis and therefore has vorticity $2\Omega\sin\phi$. This is called ***planetary vorticity***. A body of water, which is stationary relative to the earth, will then automatically possess planetary vorticity *f*. Fig. 9.16(b) shows how this quantity varies with position on the surface of the earth.

9.11.3 *Absolute vorticity—(ζ+f)*

The equations for the horizontal components of motion without friction are

$$\begin{aligned} \frac{du}{dt} - f\,v &= -\alpha\frac{\partial p}{\partial x} \\ \frac{dv}{dt} + f\,u &= -\alpha\frac{\partial p}{\partial y} \end{aligned} \tag{9.35}$$

If we cross-differentiate these equations and subtract them, to eliminate the pressure terms, we get

$$\frac{d}{dt}(\zeta + f) = -(\zeta + f)\left(\frac{\partial u}{\partial x} + \frac{\partial v}{\partial y}\right) = -(\zeta + f)\nabla\cdot\vec{V}_H \tag{9.36}$$

(1) $\nabla\cdot V_H$ will be recognized as a measure of the tendency for horizontal flow to diverge (if $\nabla\cdot\vec{V}_H$ is +) or to converge (if $\nabla\cdot\vec{V}_H$ is –).

(2) The quantity (ζ+*f*), the sum of the relative and planetary vorticities, is called the ***absolute vorticity***. Eq. (9.36) expresses the Principle of Conservation of Absolute Vorticity for flows on the earth when frictional effects are neglected.

(3) If a divergence, the magnitude of the absolute vorticity decreases with time, whereas in a convergence, the absolute vorticity magnitude increases with time.

(4) *f* is usually much larger than ζ, positive values for (f+ζ) will usually be found in the northern hemisphere and negative values in the southern.

A body of water in the form of a vertical cylinder of small height is initially stationary relative to the earth so that it has planetary vorticity *f* only.

(1) If the fluid now starts to flow inward (converges) toward the axis of the cylinder it must also elongate because volume is conserved; because $\nabla\cdot\vec{V}_H$ is negative, the absolute vorticity must increase. In this case the water will

acquire some relative vorticity ζ, so that its absolute vorticity increases from f to $(f+\zeta)$ as the cylinder shrinks and elongates (Fig. 9.17(a)).

(2) In Fig. 9.17(b) is shown the opposite situation in which a tall, narrow cylinder expands (diverges) to form a low, wide one. If its initial vorticity was simply f its final vorticity will decrease to $(f-|\zeta|)$.

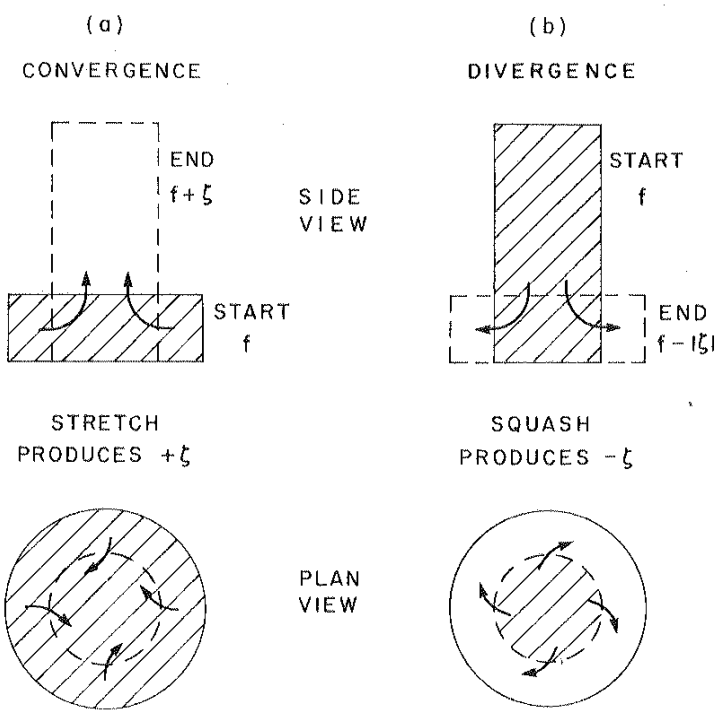

Fig. 9.17 Change of absolute vorticity associated with (a) convergence, (b) divergence (both for northern hemisphere).

9.11.4 *Potential vorticity*—$(f+\zeta)/D$

Let us consider a layer of thickness D in the sea whose density is uniform so that the horizontal velocity components are independent of depth. Then the equation of continuity of volume for the layer is

$$\frac{1}{D}\frac{dD}{dt}+\left(\frac{\partial u}{\partial x}+\frac{\partial v}{\partial y}\right)=0 \tag{9.37}$$

If we combine this equation with (9.36), eliminating the horizontal divergence term, we get

$$\frac{d}{dt}\left(\frac{\zeta+f}{D}\right)=0,\ \text{i.e.}\left(\frac{\zeta+f}{D}\right)=\text{constant} \tag{9.38}$$

for the motion of a water body in the ocean provided that there is no input of vorticity (such as might come from a wind stress or other frictional effects). The quantity $(f+\zeta)/D$ is called the ***potential vorticity*** of the water.

(1) if D remains constant

(a) then if a column of water moves zonally (along a parallel of latitude so that ϕ remains constant), then f remains constant and so must ζ;

(b) if a column of water moves meridionally (along a line of constant longitude) toward the north pole, then f automatically increases and ζ must decrease to keep $(f+\zeta)$ constant, i.e. the water acquires more negative (clockwise) rotation relative to the earth;

(c) conversely, if a column of water moves toward the south pole then it acquires more positive (anticlockwise) rotation;

(2) if D increases, then $(f+\zeta)$ must increase if it is positive initially,

(a) so if the water moves zonally, then f remains constant so ζ must increase, i.e. the water acquires more positive (anticlockwise) rotation;

(b) if the water moves meridionally toward the north pole, then f automatically increases, and it is not immediately obvious what ζ will do;

(c) if the water moves meridionally toward the south pole, f decreases and ζ must increase, i.e. the column acquires more positive (anticlockwise) rotation;

(3) if D decreases, then $(f+\zeta)$ must decrease if it is initially positive.

In the interior of the ocean, for large-scale processes, ζ is negligible compared with $f \Rightarrow f/D$ = constant. If a water column stretches (D increases) then f must increase in magnitude; the water must move toward the nearest pole, north or south. The condition f/D = constant permits us to predict which way a current will swing on passing over bottom irregularities—equatorward over ridges and poleward over troughs in both hemispheres. The deflection of the flow required to keep f/D constant is sometimes called ***topographic steering***.

9.12 Westward intensification of ocean currents explained using conservation of vorticity

Here we must include changes in vorticity due to frictional effects such as the wind, which is important in driving the upper layer.

Consider a northern hemisphere ocean with winds to the west in the south and to the east in the north, causing the upper-layer circulation to be clockwise (i.e. the angular rotation is negative).

(1) On the west side of the ocean the flow will be to the north (Fig. 9.18(a)) and the relative vorticity will become more negative (i.e. $-\zeta_p$) due to the northward movement which causes f to increase, and also more negative ($-\zeta_\tau$) due to the wind stress which provides clockwise, i.e. negative vorticity. Therefore, there is a net decrease of relative vorticity ($-\zeta_p-\zeta_\tau<0$) on the west side.

(2) On the east side (Fig. 9.18(b)) the flow is to the south and so the relative vorticity increases ($+\zeta_p$) due to the decrease of f and decreases ($-\zeta_\tau$) due to the wind stress.

(3) Sverdrup demonstrated that on the east side of the ocean, $\beta M_y = \mathrm{curl}_z\ \vec{\tau}_\eta$,

i.e. the increase and decrease terms for relative vorticity, will be about equal in the east and there will be no change during the southward flow, i.e. $+\zeta_p-\zeta_\tau \cong 0$ in the east.

(4) For the complete circulation it is necessary to supply vorticity to make up for the decrease in the west, in order to keep the total vorticity constant. One way to do so is through lateral friction on the west side only, so that the decrease of planetary vorticity and decrease of vorticity due to wind stress are made up by increase of vorticity from lateral shear in the water currents, i.e. $-\zeta_p-\zeta_\tau+\zeta_f \cong 0$.

(5) For this balance we need a vorticity structure such as in Fig. 9.18(b) where there are strong currents with much shear in the west, but slow currents with little shear in the east, i.e. westward intensification of the ocean currents.

(6) Note that there are two essential features: f must be allowed to vary with latitude (as Stommel showed) and ζ must be small compared with f.

(7) Where the wind stress causes an anticlockwise circulation (the largest ones being in the southern hemisphere), similar arguments again lead to westward intensification.

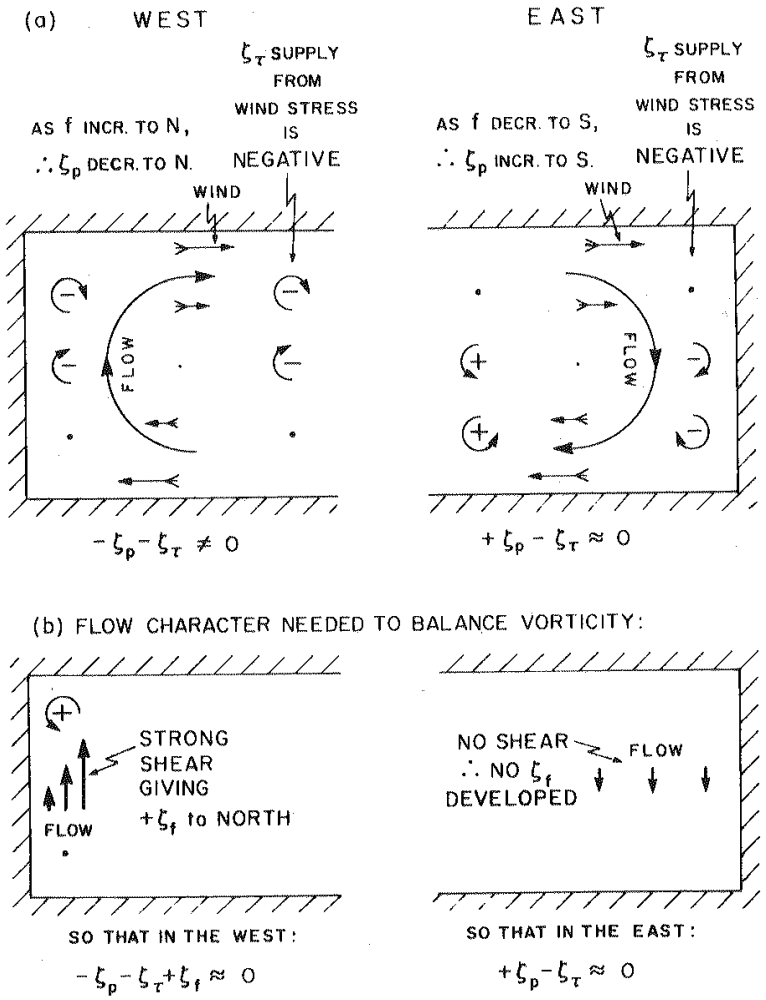

Fig. 9.18 Use of conservation of vorticity to explain western intensification of ocean currents: (a) relative vorticity supplied by wind stress, (b) relative vorticity supplied by frictional stress at boundary.

9.13 The equatorial current system

9.13.1 *The surface equatorial currents*

The equatorial current system is: zonal character with westward- following North and South Equatorial Currents and, between them, the eastward North Equatorial Countercurrent.

(1) The earliest explanation offered for the existence of the eastward Countercurrent, flows opposite to the prevailing westward winds, was that the wind stress piled up water at the west and that the Counter- current was a pressure-gradient driven flow in the zone of the “doldrums”, the weaker (through still westward) winds between the stronger Northeast and Southeast Trade Winds. Later studies showed this explanation to be inadequate.

(2) The curl of the wind-stress theory of Sverdrup has been accepted as the proper explanation, i.e. it is the meridional change of wind stress between the stronger trade winds and the weaker doldrums which is responsible rather than the smaller wind stress itself in the doldrums.

(3) In addition to these three major currents, there are other surface currents, e.g. a weaker South Equatorial Countercurrent between 5° and 10°S. There is a fourth major component of the equatorial system — the subsurface Equatorial Undercurrent.

9.13.2 *The Equatorial Undercurrent*

Beneath the surface and embedded in the westward-following Pacific South Equatorial Current there exists a most remarkable current — the Equatorial Undercurrent.

(1) This current flows eastward, centered on the equator. Maximum speeds are 1.5 ms^{-1} or more at a depth rising from 200 m in the west to 50 m or less in the east; the annual average transport has recently been estimated at about 40 Sv with maximum transports up to 70 Sv.

(2) The current is like a thin ribbon, about 0.2 km thick and 300 km wide; it can be followed for some 14,000 km across most of the Pacific.

(3) A similar current exists in the Atlantic, and was recognized in 1886 by Buchanan but his accounts were ignored.

(4) There is also evidence for an equatorial undercurrent in the Indian Ocean during the northeast monsoon period (November-March).

How do they arise? Consider first what is happening right at the equator where the Coriolis effect is zero and where there is a well-defined upper, mixed (constant density) layer above the thermocline.

(1) The wind is blowing with a westward component and the surface current is to the west. Because there are land barriers at the western side the water tends to pile up there, producing a surface slope up toward the west and therefore a pressure gradient force develops toward the east.

(2) The surface layer will tend to be thicker in the west with the thermocline (and pycnocline) sloping opposite to the surface slope, i.e. upward to the east.

(3) At some considerable depth the opposite slope of the isopycnals relative to the surface can lead to baroclinic compensation and a reduction of the

east-west pressure gradient to zero. At the surface the westward component of the wind stress can balance the eastward pressure gradient.

(4) As one goes below the surface, the stress caused by the surface wind decreases and the eastward pressure gradient can no longer be balanced by the downward momentum transfer and produces the eastward-flowing undercurrent at the bottom of the mixed layer.

(5) Because of the strong eastward current there will be frictional forces (and perhaps inertial effects), which will balance the pressure gradient and allow a steady-state flow to occur.

(6) As one goes away from the equator, Coriolis effects become important. In the surface layer with a westward-directed wind, the Ekman transport will be away from the equator on both north and south sides so there will be a surface divergence with consequent ***upwelling*** and biological production. Below the surface layer there must be convergence (flow toward the equator) to balance the surface divergence.

(7) In the about north and south of 1.5° latitude, the Coriolis force associated with this equatorward flow can balance the eastward pressure gradient. It is only very near to the equator that the Coriolis effect is so weak that the Undercurrent is possible.

(8) Although the Coriolis force vanishes at the equator, its variation with latitude ($\partial(2\Omega\sin\phi)/\partial\phi = 2\Omega\cos\phi \Rightarrow 2\Omega$ as $\phi \rightarrow 0°$) is a maximum there and tends to stabilize the current. If the eastward current wanders southward, the Coriolis force will be to the left pushing it back to the equator; if it goes northward, the Coriolis force is to the right, again bringing it back toward the equator.

(9) In fact, the variation of the Coriolis force with latitude will tend to stabilize eastward-flowing currents anywhere in the ocean and to accentuate meandering of westward-flowing currents with the strongest effects at the equator where the variation is a maximum.

(10) It is only in the long term that the Undercurrent is "tied" to the equator. Evidence for north-south oscillations in equatorial currents has been found. They are probably associated with the variation of the Coriolis effect with latitude and may be thought of as Rossby waves superimposed on the average current. These waves, which are possible because of the Coriolis effect variation, will be discussed in Chapter 12.

(11) A weakness of the constant density upper-layer models is that they predict

an undercurrent at the bottom of the mixed layer whereas observations indicate that the strongest current is actually below this in the thermocline/pycnocline region below the mixed layer.

(12) More elaborate theories, which developed from studies of temporal variations in the equatorial region, e.g. Rossby waves, and incorporate density stratification rather than a simple two-layer model, are able to describe the existence of the undercurrent in the thermocline (see Philander (1973) and Leetmaa et al. (1981)).

(13) It must be admitted that no fully satisfactory theory of the Equatorial Undercurrent is yet available.

9.14 *Boundary-layer approach*

Whenever higher-order derivatives in the equations exist but have small coefficients (such as the Rossby and Ekman numbers) we expect ***boundary layers*** to occur. These are relatively thin regions near the boundary where some of the terms with higher-order derivatives will become important. Simple equations will hold in the interior of the ocean, such as the geostrophic equations.

To use the boundary-layer approach we re-scale the equations, changing the appropriate length scale to one relevant to the boundary- layer thickness. The advantage of this approach is that only the higher- order terms which matter will become important.

9.14.1 *The use of the boundary-layer approach to obtain a solution to Munk's equation*

Here we are going to non-dimensionalize Munk's form of the vertically integrated vorticity equation. In the interior away from the western boundary, the Sverdrup balance holds.

$$\psi_i = -\frac{1}{\beta}\int \mathrm{curl}_z\ \vec{\tau}_\eta dx + C \tag{9.39}$$

where i indicates the stream function in the interior. We note that the change in the value of ψ across the western boundary must also be of the same size because the boundary current is returning the interior flow and the change in ψ in each region gives a measure of the total transport.

$$\psi = (\tau_0 / \beta)\psi' \quad \text{and} \quad \vec{\tau}_\eta = \tau_0 \vec{\tau}'_\eta \tag{9.40}$$

where the primes indicate non-dimensional variables with a range of order 1.

$$x = \xi W \qquad \text{and} \qquad y = \gamma L \tag{9.41}$$

where ξ and γ are non-dimensional variables. In the interior, W is O(L). In the western boundary, $W \ll L$ because the boundary current is long and narrow. If we substitute equation (9.40) and (9.41) into (9.34) we get

$$\frac{A\tau_0}{\beta}\left[\frac{1}{W^4}\frac{\partial^4\psi'}{\partial\xi^4} + \frac{2}{W^2L^2}\frac{\partial^4\psi'}{\partial\xi^2\partial\gamma^2} + \frac{1}{L^4}\frac{\partial^4\psi'}{\partial\gamma^4}\right] - \frac{\tau_0}{W}\frac{\partial\psi'}{\partial\xi} = \tau_0\left[\frac{1}{W}\frac{\partial\tau'_{y\eta}}{\partial\xi} - \frac{1}{L}\frac{\partial\tau'_{x\eta}}{\partial\gamma}\right]$$

Multiplying by W/τ_0 and some rearranging gives

$$\frac{A}{\beta W^3}\left[\frac{\partial^4\psi'}{\partial\xi^4} + 2\left(\frac{W}{L}\right)^2\frac{\partial^4\psi'}{\partial\xi^2\partial\gamma^2} + \left(\frac{W}{L}\right)^4\frac{\partial^4\psi'}{\partial\gamma^4}\right] - \frac{\partial\psi'}{\partial\xi} = \frac{W}{L}\left[\frac{L}{W}\frac{\partial\tau'_{y\eta}}{\partial\xi} - \frac{\partial\tau'_{x\eta}}{\partial\gamma}\right] \tag{9.42}$$

Note that

(1) $(L/W)(\partial\tau'_{y\eta}/\partial\xi)$ remains of O(1) both in the interior, where $W \cong L$, and in the boundary layer because the magnitude of $\text{curl}_z\,\vec{\tau}_\eta$ is the same in both regions.

(3) In the western boundary region where W « L and ξ changes rapidly, $\partial\tau'_{y\eta}/\partial\xi$ becomes very small, of O(W/L).

(4) Recall that $\partial\tau_{x\eta}/\partial y$ is the dominant term in the wind-stress curl everywhere, so the term coming from $\partial\tau_{y\eta}/\partial x$ cannot become important no matter how we non-dimensionalize the equation.

(5) Following Munk we take $A = 5\times10^3$ m^{2}s^{-1} and $\beta = 1.9\times10^{-11}$ m^{-1}s^{-1}. For the interior take $W = 5\times10^6$ m. Then $A/(\beta W^3) = 2\times10^{-6}$, so the friction terms are negligible and the simple Sverdrup balance holds. To make the friction terms of O(1) to balance $\partial\psi'/\partial\xi$ we must take

$$W = (A/\beta)^{1/3} = (5\times10^3/1.9\times10^{-11})^{1/3} \cong 6\times10^4 \text{ m} = 60 \text{ km}$$

This is an example of how the scaling can be used to find out how the width of the western boundary current must depend on the other parameters in the

system.

(6) Now with W = 60 km, the friction term is O(1) and so is $\partial\psi'/\partial\xi$. However, the wind-stress term is now O(W/L) or O(0.01) and may be neglected to a good approximation.

(7) With the much higher velocities and transport/unit width in the western boundary current the relatively small local wind-induced transports can be ignored. Thus in the western boundary we have, a good approximation,

$$\frac{\partial^4\psi'}{\partial\xi^4} - \frac{\partial\psi'}{\partial\xi} = 0 \tag{9.43}$$

The use of the boundary layer approach has simplified equation (9.34) to (9.43) which shows the strength of the method.

Eq. (9.43) has a unique simple solution as

$$\psi' = C_0 + \sum_{n=1}^{n=3} A_n \exp(a_n\xi) \tag{9.44}$$

where $a_1 = 1, a_2 = -1/2 + i\sqrt{3}/2, a_3 = -1/2 - i\sqrt{3}/2$. Now A_1 = 0 must be chosen because exp(ξ) is divergent as ξ becomes large. The solution with a_1 = 1 can be used on the eastern boundary to satisfy the no-slip condition as we shall show presently. Using ψ=0 (no flow through the boundary) and $\partial\psi/\partial x$=0 (M_y=0 or no slip or flow along the boundary) at x=0 determines A_2 and A_3 and we have

$$\begin{aligned}\psi' &= C_0\left[1 - \exp(-\xi/2)\left(\cos\left(\sqrt{3}\xi/2\right) + \frac{\sin\left(\sqrt{3}\xi/2\right)}{\sqrt{3}}\right)\right] \\ &= C_0 T(\xi)\end{aligned} \tag{9.45}$$

$T(\xi)$ goes to 1 as ξ becomes very large (as we go from the boundary layer to the interior).

Thus $\psi' \to C_0$ as we move to the interior and, in dimensional units, C_0 must be the value of the interior transport stream-function at the edge of the boundary layer. Because W/L«1, we can, to a good approximation, use ψ_i at x=0. Thus $\psi = \psi_i(x,y)T(x/W)$ and from before

$$\psi_i = -\frac{1}{\beta}\int_0^x \mathrm{curl}_z\vec{\tau}_\eta\, dx + C$$

Using ψ_i=0 at x=L, the eastern boundary, gives

$$C = \frac{1}{\beta}\int_0^L \mathrm{curl}_z\vec{\tau}_\eta\, dx \qquad \text{and finally}$$

$$\psi = \left(\frac{1}{\beta} \int_x^L \mathrm{curl}_z \vec{\tau}_\eta \, dx \right) T(x/W) \tag{9.46}$$

where $T(x/W)$ is given by the expression multiplying C_0 in (9.45) with ξ replaced by x/W. To complete the solution fully, we add to the right-hand side of (9.46) the quantity

$$(W'/\beta)(\mathrm{curl}_z \vec{\tau}_\eta)_{x=L} \left[\exp\{(x-L)/W'\} - T(x/W) \right]$$

which is negligible except near the eastern boundary and which makes $\partial\psi/\partial x$ vanish at $x=L$. W' is an eastern boundary width and $W' \ll L$. Since A in the eastern boundary will probably be smaller than in the west, friction probably being weaker here, W' (proportional to $A^{1/3}$) is likely to be smaller than W of the western boundary.

Now from the solution, the actual width of the western boundary current is 3 to 4 times $(A/\beta)^{1/3}$ or, for the values chosen by Munk, about 200 km. The width is probably reasonable for the climatological average Gulf Stream or Kuroshio. However, at any one time these streams are only 50–60 km wide. Using the Munk theory with $A = (\beta W^3)$ suggests for the short-term average stream that A is of order 10^2 $\mathrm{m^2 s^{-1}}$. Now the inertial or non-linear terms are of order $10^3/A=10$ times the turbulent friction terms. Thus for the short-term average western boundary current, inertial or non-linear effects are probably not negligible.

9.14.2 *A simple inertial theory by Stommel; the Rossby radius of deformation*

This is an idealized model used to see if a predominantly inertially controlled Gulf Stream is a reasonable approximation. Stommel assumes a two-layer system. The upper layer has density ρ_1 and is moving; the lower layer has density ρ_2 and is at rest. The thickness of the upper layer, D, is 0 at the coast (x=0) and increases to D_0 at the outer edge of the western boundary layer. The x–axis is taken across the stream and the y–axis along it.

The pressure in the lower layer

$$p = -\int_\eta^z \rho \, g \, dz = -\int_\eta^d \rho_1 g dz - \int_d^z \rho_2 g dz$$

where η is the surface elevation from the rest state with z=0 at the surface and d is the level of the interface between the layers measured from the z = 0 reference. Now ρ_1 and ρ_2 are constants and may be taken outside the integrals giving

$$p = \rho_1 g(\eta - d) + \rho_2 g(d - z) = \rho_1 g \eta + (\rho_2 - \rho_1) g d - \rho_2 g z$$

Then $\frac{\partial p}{\partial x} = \rho_1 g \frac{\partial \eta}{\partial x} + (\rho_2 - \rho_1) g \frac{\partial d}{\partial x}$ in the lower layer.

But in this layer there is no flow (by assumption) and therefore the horizontal pressure force must be zero, i.e.

$$\frac{\partial d}{\partial x} = -\frac{\rho_1}{\rho_2 - \rho_1} \frac{\partial \eta}{\partial x}$$

If we wish to use the total upper layer thickness, taken to be positive, $D = \eta - d$ and

$$\frac{\partial D}{\partial x} = \frac{\partial \eta}{\partial x} - \frac{\partial d}{\partial x} = \left(1 + \frac{\rho_1}{\rho_2 - \rho_1}\right) \frac{\partial \eta}{\partial x} = \left(\frac{\rho_2}{\rho_2 - \rho_1}\right) \frac{\partial \eta}{\partial x}$$

(1) Now $(\rho_2 - \rho_1) \ll \rho_1$, e.g. in the Gulf Stream $(\rho_2 - \rho_1) \cong 2\times10^{-3}\rho_1$. Thus the slope of the interface is much larger than the slope of the surface and is of the opposite sign.

(2) In more general case of continuous density variation, the results would be similar to that for an idealized two-layer system. If the horizontal pressure gradients go to zero at depth, the isopycnal slopes will be mainly opposite to the surface slope and much larger.

In the upper layer above $z = d$

$$p = \rho_1 g(\eta - z) \quad \text{and} \quad \frac{\partial p}{\partial x} = \rho_1 g \frac{\partial \eta}{\partial x}$$

The x–momentum equation remains geostrophic to a good approximation as

$$-f v = -\frac{1}{\rho_1} \frac{\partial p}{\partial x} = -\frac{\rho_2 - \rho_1}{\rho_2} g \frac{\partial D}{\partial x} = -g' \frac{\partial D}{\partial x} \qquad (9.47)$$

where $g' = g(\rho_2 - \rho_1)/\rho_2$ is termed the ***"reduced gravity"***. The total transport of the stream is $Q = \int_0^W Q_y dx$ where W is the value of x at the seaward edge of the stream. As the upper layer is homogeneous, v is independent of depth within the upper layer and zero below it, so $Q_y = vD$. Using (9.47) gives

$$Q = \int_0^w \frac{g'}{f} D \frac{\partial D}{\partial x} dx = \int_0^w \frac{g'}{f} \frac{1}{2} \frac{\partial D^2}{\partial x} dx = \frac{g'}{f} \frac{D_0^2}{2}$$

since $D = 0$ at $x = 0$ and $D = D_0$ at $x = W$.

(1) Following Stommel we assume that the potential vorticity is essentially constant. This assumption should be valid if friction effects are small

enough to be neglected.

(2) The important inertial terms are retained. Observations in the Gulf Stream do show that the potential vorticity remains nearly constant.

(3) For the relative vorticity $\partial u/\partial y$ is negligible compared with $\partial v/\partial x$ both because $v \gg u$ and because the Stream is long and narrow. Thus constant potential vorticity reduces to $(f + \partial v/\partial x)/D$ = constant = f/D_o since at the "edge" of the Stream $\partial v/\partial x$ will be small.

Rossby Radius of Deformation

The Rossby radius of deformation λ is the horizontal scale at which rotation effects become as important as buoyancy effects.
The Gulf Stream example:

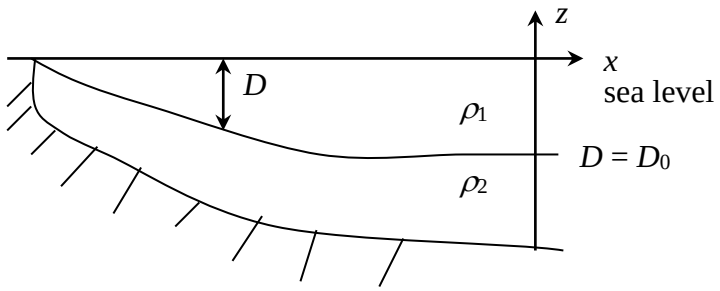

Conservation of potential vorticity (assuming friction is negligible) is:

$$\frac{d}{dt}\left(\frac{\varsigma + f}{D}\right) = 0$$

For the Gulf Stream: $v \gg u$ and $x \ll y$ so, $\varsigma = \dfrac{\partial v}{\partial x} - \dfrac{\partial u}{\partial y} \approx \dfrac{\partial v}{\partial x}$

$$\frac{d}{dt}\left[\frac{1}{D}\left(\frac{\partial v}{\partial x} + f\right)\right] = 0$$

$$\frac{1}{D}\left(\frac{\partial v}{\partial x} + f\right) = \text{constant} = \frac{f}{D_0}$$

because $\partial v/\partial x = 0$ at the eastern edge of the Gulf Stream, where $D = D_0$.
Taking $\partial/\partial x$ of (9.47) and substituting for $\partial v/\partial x$ in the potential vorticity equation gives

$$\left(f + \frac{g'\partial^2 D}{f\partial x^2} \right) / D = f / D_0. \quad \text{Rearrangement gives} \quad \frac{\partial^2 D}{\partial x^2} = \frac{(D - D_0)}{\lambda^2}$$

where $\lambda = \sqrt{(g'D_0)} / f$ is called the ***Rossby radius of deformation*** and gives a length scale based on the parameters of the system. (Since it depends on density differences, λ is completely termed an ***internal*** radius of deformation (λ_i); the ***external*** radius of deformation ($\lambda_e = \frac{\sqrt{gD_0}}{f}$) is defined in section 12.10.3 and compared with the internal radius.) the solution is

$$D = D_0[1 - \exp(-x/\lambda)], \quad v = \sqrt{g'D_0}\exp(-x/\lambda)$$

With D_o = 800 m, f = 10^{-4} s^{-1}, and $(\rho_2 - \rho_1)/\rho_2 \cong 2 \times 10^{-3}$, $Q \cong$ 63 Sv and the maximum value of v = 4 ms^{-1}. Also λ = 40 km which gives a length scale for the "width" of the Stream.

(1) The simple inertial boundary layer model gives a transport similar to that from observations for the northeastward flow of the Gulf Stream and, in the outer part of the Stream, the velocity calculated from the model solution fits the velocity calculated using the geostrophic equation and observations of temperature and salinity reasonably well.

(2) Near the inshore edge, the observed velocity decreases whereas the model velocity continues to increase.

(3) While the model is too simple to represent the Gulf Stream in detail it does indicate that inertial effects need to be included, particularly on the outer side of the Stream south of where the transport is a maximum. On the inshore edge, friction probably becomes important and beyond the latitude of maximum transport the stream shows much more meandering so a more complicated model is needed.

Interpretation of Rossby Radius:

$\sqrt{gD_0}$ = velocity of a shallow water wave

$\sqrt{g'D_0}$ = velocity of a shallow water internal wave

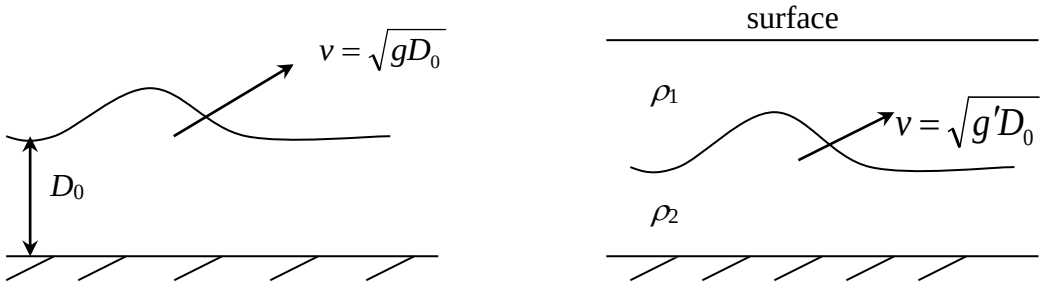

Distance = velocity × time = $\frac{\sqrt{g'D}}{f}$ or $\frac{\sqrt{gD}}{f}$

Hence, Rossby radius is closely associated with the adjustment of geostrophic flow to transient. Also, Rossby radius gives typical size of oceanic eddies:

Eddy size $L = \sqrt{g'D}\,T = \sqrt{g'D}\,\frac{2\pi}{f} = 2\pi\lambda \approx 240\,\text{km}$ in the Gulf Stream

For $x \ll \lambda$, rotation effects are small. $x \geq \lambda$, rotation is important.